
ΕΘΝΙΚΟ ΜΕΤΣΟΒΙΟ ΠΟΛΥΤΕΧΝΕΙΟ

ΔΠΜΣ «ΥΠΟΛΟΓΙΣΤΙΚΗ ΜΗΧΑΝΙΚΗ»

# Μαθηματική μοντελοποίηση μετάδοσης COVID-19 σε εσωτερικό χώρο

---

ΜΕΤΑΠΤΥΧΙΑΚΗ ΕΡΓΑΣΙΑ

Ρεντούμης Ιωάννης

Επιβλέπων Καθηγητής: Φούντη Μαρία

Καθηγητής Ε.Μ.Π.

Υπόψη: Νίκου Μαρκάτου

Ομότιμου Καθηγητή ΕΜΠ

ΑΘΗΝΑ, 2021

# ΠΕΡΙΛΗΨΗ

Ο ιός COVID-19 που εμφανίστηκε πρώτη φορά σε μια υπαίθρια αγορά της Ουχάν στην Κίνα τον Δεκέμβριο του 2019, πολύ σύντομα μεταδόθηκε σε όλον το κόσμο. Τον Ιανουάριο πολλές μεγάλες ευρωπαϊκές χώρες απομάκρυναν τους υπηκόους τους από την Κίνα, ανοίγοντας την δίοδο στον ιό προς την Ευρώπη. Η πανδημία έχει κηρυχθεί από τον Παγκόσμιο Οργανισμό Υγείας (Π.Ο.Υ.) ως «Έκτακτη Ανάγκη Δημόσιας Υγείας Διεθνούς Ενδιαφέροντος» (PHEIC) στις 30 Ιανουάριου 2020.

Με γνώμονα την προστασία της δημόσιας υγείας και την αποτροπή διασποράς του κορονοϊού SARS-COV-2, οι κυβερνήσεις ανά τον κόσμο προχώρησαν στη λήψη έκτακτων μέτρων όσον αφορά τη λειτουργία των δημοσίων υπηρεσιών. Η απόσταση μεταξύ ατόμων τέθηκε το ελάχιστο 1,5 μέτρα.

Η παρούσα διπλωματική εργασία έχει ως στόχο να αξιολογήσει την ασφαλή απόσταση μεταξύ ατόμων, που έχει τεθεί από τους κανονισμούς σε δημοσίους χώρους. Παράλληλα πρέπει να διαπιστωθεί εάν έχουν ληφθεί υπόψιν οι παράγοντες που μπορεί να μεταφέρουν αιωρούμενα μολυσμένα σωματίδια. Τέτοιοι παράγοντες μπορεί να είναι η ταχύτητα του ανέμου σε ένα εξωτερικό χώρο, η ταχύτητα ενός ατόμου ξενιστή, για παράδειγμα την ώρα που αυτός τρέχει, ή στην προκειμένη περίπτωση το πώς μεταφέρονται τα σωματίδια όταν αυτά επηρεάζονται από ένα σώμα κλιματισμού. Πιο συγκεκριμένα στην παρούσα εργασία μελετήθηκε η διασπορά του ιού από φτέρνισμα και βήχα ενός ατόμου και πως τα αιωρούμενα σωματίδια επηρεάζονται από την ταχύτητα του ανέμου του κλιματιστικού σώματος. Δύο μοντέλα δημιουργήθηκαν, το πρώτο μοντέλο προσομοίωνε έναν μεγάλο χώρο σουπερμάρκετ με παράθυρα και πόρτες, εστιάζοντας σε μια πολυπαραγοντική προσέγγιση. Σε αντίθεση, το δεύτερο χωρίο είναι μικρότερο σε μέγεθος, χωρίς παράθυρα και με μια πόρτα έτσι ώστε οι υπόλοιποι παράγοντες να έχουν μικρότερη δράση. Στην ουσία η κεντρική διαφορά των δυο μοντέλων είναι ότι το δεύτερο εστιάζει σε έναν χώρο με λιγότερες μεταβλητές. Επιπροσθέτως, διεξήχθη έρευνα για έναν ασυμπτωματικό ασθενή με σκοπό να εξεταστεί η ασφάλεια της απόστασης του 1,5 μέτρου. Διότι, τα σταγονίδια που εκπνέει ο ασυμπτωματικός ασθενής μπορούν να μεταφερθούν σε μεγαλύτερη απόσταση μέσα στο δωμάτιο. Κατά συνέπεια μπορεί να εξεταστεί

εάν η απόσταση του 1,5 μέτρου είναι τόσο σημαντική όσο η μακρόχρονη παραμονή του ατόμου στο φορτισμένο με ιικό φορτίο δωμάτιο. Μελλοντικές έρευνες θα μπορούν να επικεντρωθούν στο χρόνο παραμονή στο δωμάτιο και όχι στις αποστάσεις.

Τα αποτελέσματα μπορούν να βοηθήσουν στον ορισμό μιας απόστασης ασφαλείας η οποία μπορεί να εφαρμοστεί σε χώρους συνάθροισης όπως για παράδειγμα: τράπεζες, εστιατόρια, χώροι διασκέδασης και αλλά.


National Technical University of Athens

MSc: Computational Mechanics

# CFD analysis of COVID-19 spread in internal environment

---

Master Thesis

Rentoumis Ioannis

Supervisor: Founti Maria

Professor NTUA

For the attention of: Nicolas Markatos

Professor Emeritus NTUA

Athens, 2021

## ABSTRACT

COVID-19 has had destructive consequences for health, economy and has altered every aspect of everyday human activity. The outbreak was first identified in December 2019 in Wuhan, China. The declaration of the disease as a "Public Health Emergency of International Concern" for the World Health Organization took place on January 30, 2020. Public distancing in internal environments has been applied as a safety measure to prevent transmission. A controversial topic is the safe distance from person to person.

The social distancing regulation, for internal public places, has been arbitrarily defined ignoring the potential aerodynamics effects of inlets, such as air-conditioning units, windows and doors. The velocity of the intake airflow has the potential to transfer a droplet from the nose or the mouth of a patient in greater than the indicated distance. The present study focuses on a model of a supermarket that includes a ventilation system and open doors.

For the transmission of COVID-19 in an air-conditioned internal space, two cases are investigated. The first design is bigger and has many doors, windows, ventilation units. On the contrary the second design is smaller and has only one door. The purpose that the two designs serve is to examine the differences in results of a multivariable internal environment (design 1) in contrast to a smaller and less affected by the included elements environment (design 2).

The numerical results obtained are compared with those obtained by two well-known empirical models related to the effective velocity of incoming air and the virus concentration. It is concluded that the computational results obtained in the present study are in acceptable agreement with those obtained by simple empirical models, especially when the standard k-ε model of turbulence is used. Thus, for the cases of coughing and sneezing patients, where we studied the largest particles that sediment onto the floor, the 6-foot rule applies well. However, pathogen-laced particles, coming for example from asymptomatic patients travel through the air indoors when people breathe and talk. Therefore, there is no much benefit to the 6-foot rule because the air a person is breathing tends to rise and comes down elsewhere, so the person is more exposed to the average background than to a person at a distance. Future research should

concentrate rather on the amount of time spent inside rather than distances. Finally, the mathematical model developed is flexible and may be easily applied to any internal air-conditioned or not environment where many people meet (e.g. banks, retail shops, restaurants, etc.) in order to provide information and useful guidelines for social distancing in times of pandemia.

# Table of Contents

# 1. Introduction

Even though the transmission rate in China, the country of origin of Covid-19 has been reduced, there are several other countries around the globe that are struggling to contain the disease. Research has shown that this disease is transmitted though saliva, in the form of small droplets produced by sternutation and coughing [1]. Therefore, there may be airborne infection due to pathogen matter in the form of small particles that disseminate the virus, spreading through large areas as aerosols [2]. Aerosols formed from persons infected with SATS-CoV-2 have the potential, under experimental circumstances, to remain viable and infectious for hours [3]. Even though those tests were conducted at laboratory environments there is enough evidence to demonstrate virus aerosols transmitting potential. To avoid the transmission, social distancing measures have been taken and are in effect, which restrict congestion in public places and define a safe distance from person to person. Although different safe distance measures have been applied around the globe, the most common one is the 1.5 m distance [4]. Thus, it has been shown that the majority of droplets are landing to the ground or they evaporate before reaching the distance of 1.5 m. Unfortunately, real internal environments that always include doors, windows and other elements such as desks, chairs and various working units, all of which are altering the aerodynamics characteristics, have not been taken into account. Furthermore, the air-conditioning in most public spaces strongly affects the air-change rate and the temperature stratification in the interior of a building [5].

The purpose of the present work is to test the validity of the simple empirical models and to provide a flexible prediction tool for more sophisticated guidelines concerning safe distances among people in public spaces of realistic configurations. The computational tool is demonstrated by applying it to a large air-conditioned supermarket, for two design cases.

As a reference for the outcome of this thesis in figure 1 it depicted the current safe distance given by Greece's heath committee. In most public places the safe distance has been defined to 1.5 m.

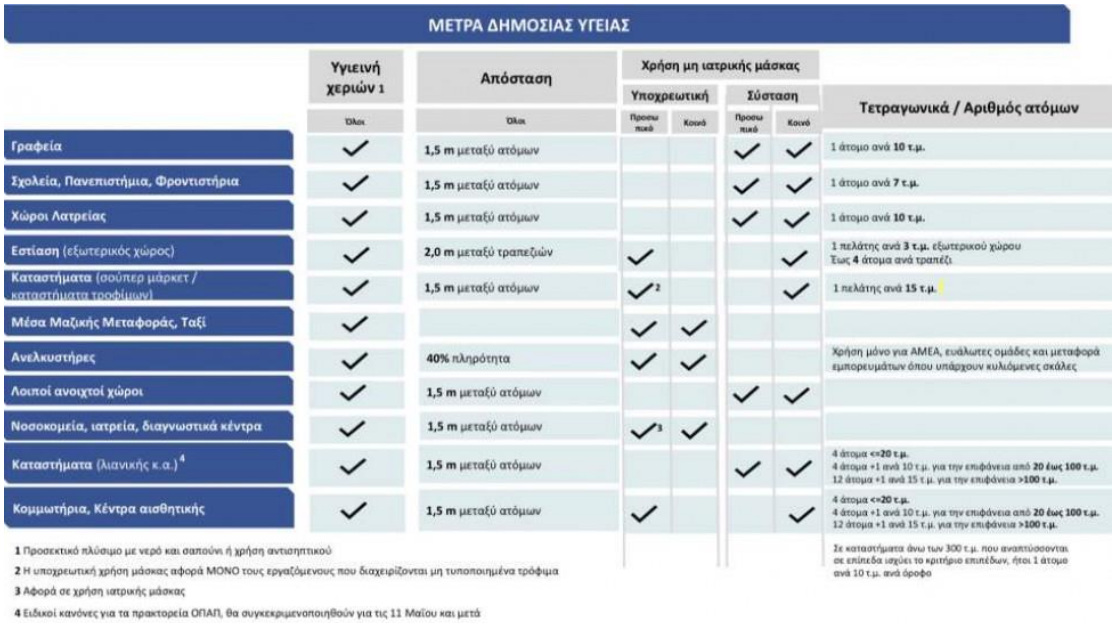

**ΜΕΤΡΑ ΔΗΜΟΣΙΑΣ ΥΓΕΙΑΣ**

| | Υγιεινή χεριών 1 | Απόσταση | Χρήση μη ιατρικής μάσκας | | | | Τετραγωνικά / Αριθμός ατόμων |
|---|---|---|---|---|---|---|---|
| | | | Υποχρεωτική | | Σύσταση | | |
| | Όλοι | Όλοι | Προσωπικό | Κοινό | Προσωπικό | Κοινό | |
| Γραφεία | ✓ | 1,5 m μεταξύ ατόμων | | | ✓ | ✓ | 1 άτομο ανά **10** τ.μ. |
| Σχολεία, Πανεπιστήμια, Φροντιστήρια | ✓ | 1,5 m μεταξύ ατόμων | | | ✓ | ✓ | 1 άτομο ανά **7** τ.μ. |
| Χώροι Λατρείας | ✓ | 1,5 m μεταξύ ατόμων | | | ✓ | ✓ | 1 άτομο ανά **10** τ.μ. |
| Εστίαση (εξωτερικός χώρος) | ✓ | 2,0 m μεταξύ τραπεζών | ✓ | | | ✓ | 1 πελάτης ανά **3** τ.μ. εξωτερικού χώρου<br>Έως **4** άτομα ανά τραπέζι |
| Καταστήματα (σούπερ μάρκετ / καταστήματα τροφίμων) | ✓ | 1,5 m μεταξύ ατόμων | ✓[2] | | | ✓ | 1 πελάτης ανά **15** τ.μ. |
| Μέσα Μαζικής Μεταφοράς, Ταξί | ✓ | | ✓ | ✓ | | | |
| Ανελκυστήρες | ✓ | **40%** πληρότητα | ✓ | ✓ | | | Χρήση μόνο για ΑΜΕΑ, ευάλωτες ομάδες και μεταφορά εμπορευμάτων όπου υπάρχουν κυλιόμενες σκάλες |
| Λοιποί ανοιχτοί χώροι | ✓ | 1,5 m μεταξύ ατόμων | | | ✓ | ✓ | |
| Νοσοκομεία, ιατρεία, διαγνωστικά κέντρα | ✓ | 1,5 m μεταξύ ατόμων | ✓[3] | ✓ | | | |
| Καταστήματα (λιανικής κ.α.)[4] | ✓ | 1,5 m μεταξύ ατόμων | | | ✓ | ✓ | 4 άτομα **<=20** τ.μ.<br>4 άτομα +1 ανά 10 τ.μ. για την επιφάνεια από **20 έως 100** τ.μ.<br>12 άτομα +1 ανά 15 τ.μ. για την επιφάνεια **>100** τ.μ. |
| Κομμωτήρια, Κέντρα αισθητικής | ✓ | 1,5 m μεταξύ ατόμων | ✓ | | | ✓ | 4 άτομα **<=20** τ.μ.<br>4 άτομα +1 ανά 10 τ.μ. για την επιφάνεια από **20 έως 100** τ.μ.<br>12 άτομα +1 ανά 15 τ.μ. για την επιφάνεια **>100** τ.μ. |

**1** Προσεκτικό πλύσιμο με νερό και σαπούνι ή χρήση αντισηπτικού

**2** Η υποχρεωτική χρήση μάσκας αφορά ΜΟΝΟ τους εργαζόμενους που διαχειρίζονται μη τυποποιημένα τρόφιμα

**3** Αφορά σε χρήση ιατρικής μάσκας

**4** Ειδικοί κανόνες για τα πρακτορεία ΟΠΑΠ, θα συγκεκριμενοποιηθούν για τις 11 Μαΐου και μετά

Σε καταστήματα άνω των 300 τ.μ. που αναπτύσσονται σε επίπεδα ισχύει το κριτήριο επιπέδων, ήτοι 1 άτομο ανά 10 τ.μ. ανά όροφο

*Figure 1 – Safety measurement from Greece Health Committee (4 May 2020)*

## 2. The physical problem considered and modeling assumptions made

As an example of mathematically modeling a public place contaminated by a virus a supermarket was chosen in two different designs. Design 1 is intended to simulate a large supermarket with many inlets and outlets. Furthermore, two people have been placed with 1.5 m between them, facing each other. On the other hand, design 2 is intended to simulate a smaller building, with less variables and there is only one human model as a patient. Comparison can be made between the two models, as the first is centralized on a multivariable environment. The second human model acting as blockage for a more realistic approach of the concentration level at 1,5 m. On the contrary, design 2 has less inlet and outlet that will alter the end result even more, the second human model is absent purposely as further distance than 1,5 m can be researched. In the present study, a ventilated public place was investigated through numerical simulation of the air-flow and the spreading of virus contaminated particles. The supermarket consists of doors, ventilation on the ceiling, air-condition units on the two sides, stacks, cash desk and the persons. The assumptions made for the problem are the following: (a) steady-state simulation of incompressible flow of a Newtonian fluid, (b) adiabatic walls, (c) constant air properties at 298.5 K, and (d) the COVID-19 droplets have been modeled in the form of concentration though the air.

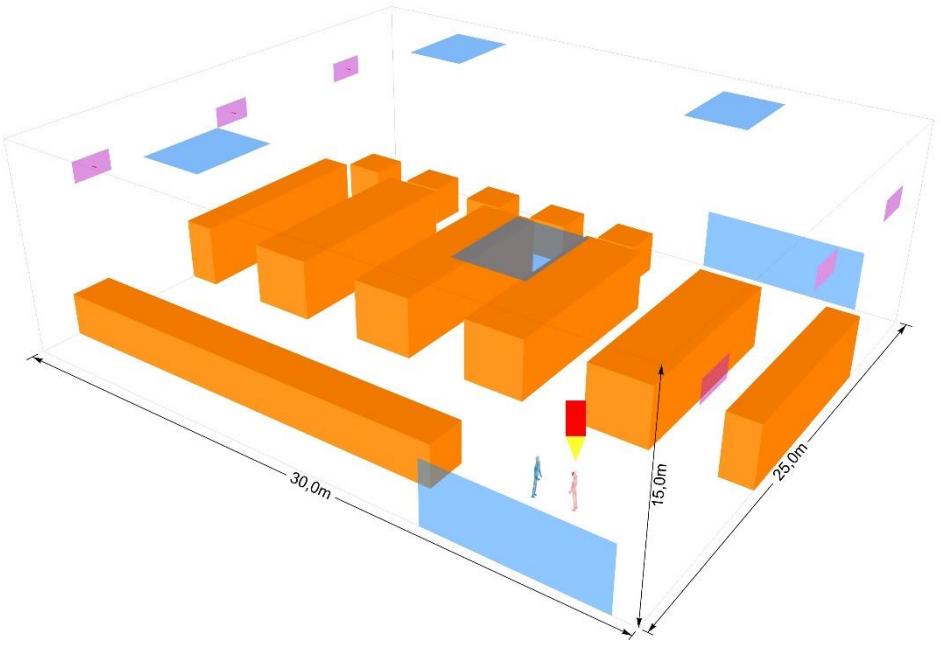


(a)

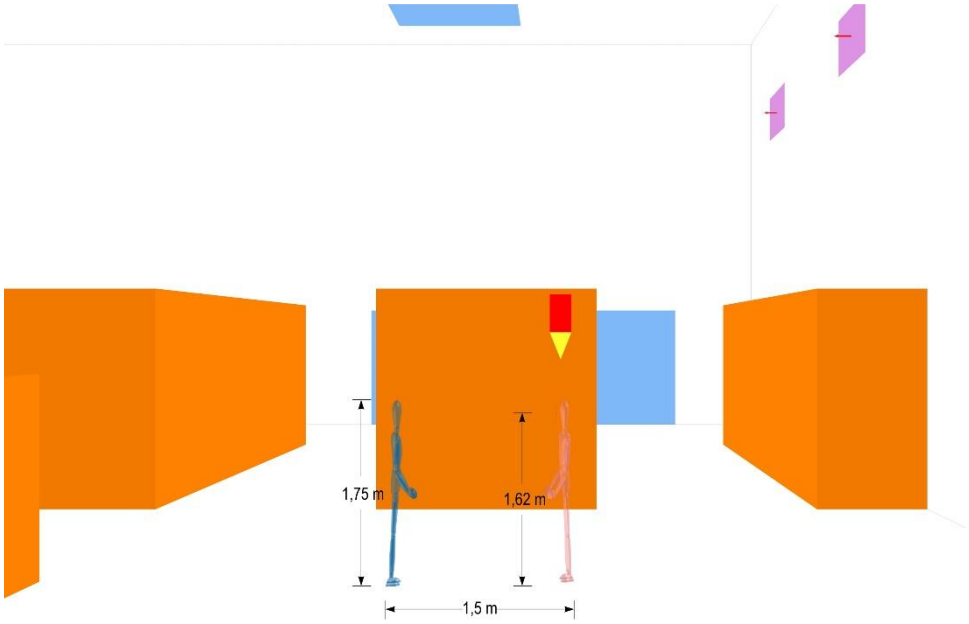


(b)

*Figure 2 - Dimension of the design1: (a) overall internal geometry, (b)the human models*

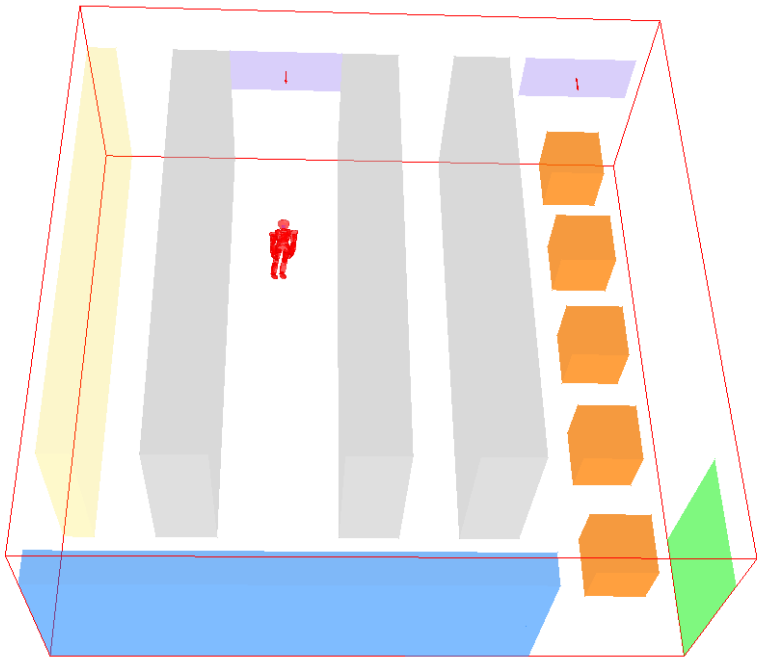

(a)

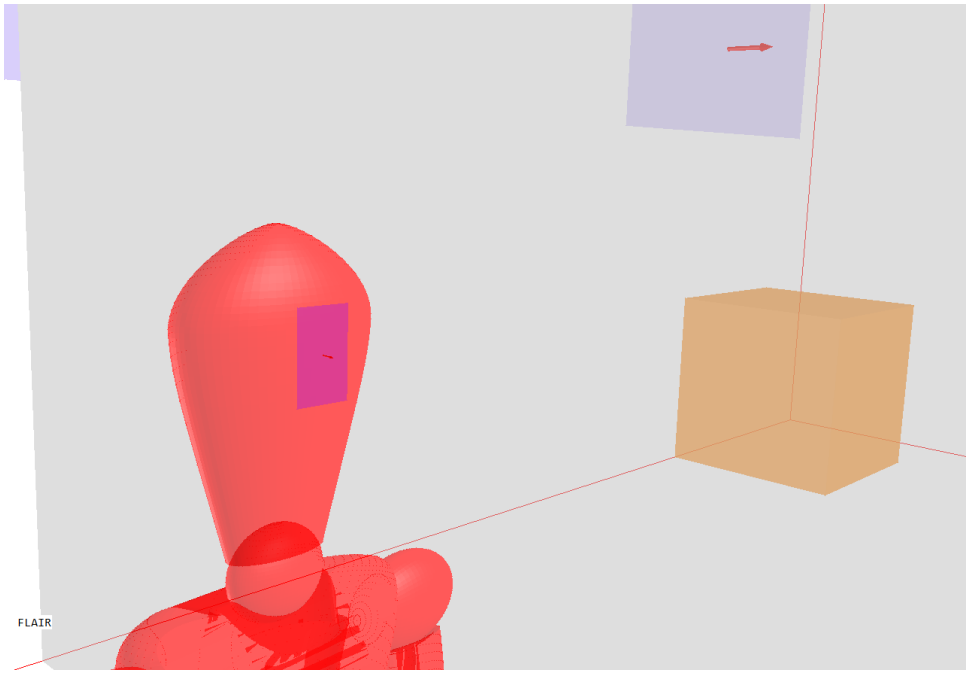


(b)

*Figure 3 - Dimension of the design 2: (a) overall internal geometry, (b) the model's facial area*

# 3. Mathematical modeling

## 3.1. Domain Properties and sizing

The domain's size and also the objects have been listed in Table 1.

*Table 1 - Domain and objects sizes in millimeter (mm)*

| | Design 1 | | | | Design 2 | | | |
|---|---|---|---|---|---|---|---|---|
| | Number | Height | Length | Width | Number | Height | Length | Width |
| Domain | - | 10500 | 25000 | 25000 | - | 4000 | 1000 | 1000 |
| Person | 2 | 1750 | 300 | 500 | 1 | 1750 | 300 | 500 |
| Mouth/Nose | 1 | 200 | 100 | - | 1 | 80 | 50 | - |
| Wall A/C | 6 | 1000 | 2000 | - | 2 | 1000 | 2000 | - |
| Door | 2 | 3000 | 8000 | - | 1 | 3000 | 2000 | - |
| Roof Ventilation | 6 | - | 4000 | 3000 | - | - | - | - |

## 3.2. Governing differential equations and turbulence models

In the steady – state problem, the independent variables are the three components (*x, y, and z*) of a Cartesian coordinate system. The flow can be characterized using the three velocity components (u, v, w), pressure p, enthalpy he, kinetic energy of turbulence, and the kinetic energy dissipation rate ε.

Apart from pressure, all these dependent variables appear as the subjects of the following general form equation:

$$\frac{\partial(\rho\varphi)}{\partial t} + div\left(\rho\vec{u}\varphi - \Gamma_{\varphi} grad\varphi\right) = S_{\varphi} \qquad (3.1)$$

where $\varphi$: The dependent variable, e.g. velocity components in three directions ($u$, $v$, $w$) , enthalpy ($h_e$), $k$ and $\varepsilon$, or 1 for the continuity equation.

ρ: Fluid density

$\vec{u}$ : Velocity vector

$\Gamma_{\varphi}$: The "effective" exchange coefficient of φ

$S_{\varphi}$: Source/Sink rate per unit volume

Making the assumption that flow takes place under steady – state conditions, the general conservation equation (3.1) for all dependent variables becomes:

$$div\left(\rho\vec{u}\varphi - \Gamma_{\varphi} grad\varphi\right) = S_{\varphi} \qquad (3.2)$$

The pressure variable is associated with the continuity equation. This leads to the so-called pressure- correction equation, which is deduced from the finite – domain form of the continuity equation. Further details may be found in literature (for example [x]).

Two turbulence models were used in the present work, in combination with the Boussinesq approximation for buoyancy effects: The RNG k-ε model and the Chen-Kim k-ε model appropriately modified to account for buoyancy forces [y].

Use is made of the logarithmic "wall functions" near solid surfaces ($11.5 < y^+ < 150$, where $y^+$ is the dimensionless distance of the first grid-node from the wall) [z].

Several runs were conducted using variable density (as a perfect-gas-law function of temperature, as an isentropic function, as a Noble-Abel correlation), to test the validity of the Boussinesq approximation. The results show that the validity of the latter is adequate.

### 3.3. Numerical solution of equations

To solve the above set of equations a numerical procedure is used based on the Finite- Volume Method (FVM) as provided by a general CFD code, i.e. PHOENICS 2019 [6]. The basic concept of this method is to discretize the space dimensions (and time also when necessary) into finite intervals and compute the variables correspondingly at only a finite number of points in three – (or four-) dimensional space. These points are usually called "grid points". The connection between the selected variables is expressed by algebraic equations, derived from their differential counterparts by integration over the control volumes defined by the above-mentioned intervals, spatial and time when required, applying the first order upwind scheme for the terms of convection.

### 3.4. Turbulence models used

For the following calculation four turbulence different models were used. Afterwards the results of each one was compared. The turbulence models used:

- k – ω
- Standard k – ε
- RNG k – ε
- Chen – Kim k – ε

In the following segments a short reference will be made.

#### 3.4.1. k-ω turbulence model

k-ω turbulence model was introduced by Wilcox[7,8] in 1988. Is a widely used two equation turbulence model. The first variable "k" being the turbulence kinetic energy and the second "ω" being the specific rate of dissipation (or turbulence frequency). That is used as an approximation for the Raynolds- averaged Navier-Stokes equations also known as the abbreviation with the letters RANS. This model makes possible the accurate near wall calculation. Furthermore, this model has shown good results in low-Reynolds number flows and at flows that separate from solid surfaces. On the other hand, the predicted flow separation can be calculated earlier than in real conditions.

The conservative form of the two-equation k-ω model is given by the following:

$$\frac{\partial}{\partial t}(\rho k) + \frac{\partial}{\partial x_j}\left(\rho k u_j\right) = \tau_{ij}\frac{\partial u_i}{\partial x_j} - \beta^* \rho k \omega + \frac{\partial}{\partial x_j}\left[(\mu + \sigma_k \mu_t)\frac{\partial k}{\partial x_j}\right] \tag{3.3}$$

$$\frac{\partial}{\partial t}(\rho \omega) + \frac{\partial}{\partial x_j}\left(\rho u_j \omega\right) = \alpha \frac{\omega}{k}\tau_{ij}\frac{\partial u_i}{\partial x_j} - \beta \rho \omega^2 + \frac{\partial}{\partial x_j}\left[(\mu + \sigma_\omega \mu_t)\frac{\partial \omega}{\partial x_j}\right] \tag{3.4}$$

*The turbulence eddy viscosity is computed from:*

$$\mu_t = \frac{\rho k}{\omega} \tag{3.5}$$

*The variables that are used in the equations (3.4) and (3.5) are as following:*

$$\alpha = \frac{5}{9} \quad \beta = 0.075 \quad \beta^* = 0.09 \quad \sigma_k = \sigma_\omega = 0.5 \tag{3.6}$$

### 3.4.2. Standard k-ε turbulence model

The k-ε model is commonly used to simulate mean flow characteristics for turbulence flow conditions in computational fluid dynamics (CFD). Unlike the mixing length model [9], the k-ε models specify both the length and velocity scale of turbulence with transport equations. (In books and papers, the phrase "turbulence kinetic energy" can be also referred as "turbulent kinetic energy"). The k-ε model was introduced in 1968 be the Harlow and Nakayama. In two-dimensional thin shear layers, the flow direction has so moderate transpose that the turbulence can adjust itself to local conditions. In flows where convection and diffusion cause significant differences between production and destruction of turbulence, e.g., in recirculating flows, a compact algebraic prescription for the mixing length is no longer feasible [10]. For turbulent kinetic energy *k*, *the* equation follows:

$$\frac{\partial}{\partial t}(\rho k) + \frac{\partial}{\partial x_j}(\rho k u_j) = \frac{\partial}{\partial x_j}\left[\left(\mu + \frac{\mu_t}{\sigma_k}\right)\frac{\partial k}{\partial x_j}\right] + P_k + P_b - \rho\varepsilon - Y_M + S_k \qquad (3.7)$$

For the dissipation rate $\varepsilon$ *of the turbulent kinetic energy*, *the* equation has as follows:

$$\frac{\partial}{\partial t}(\rho\varepsilon) + \frac{\partial}{\partial x_j}(\rho\varepsilon u_j) = \frac{\partial}{\partial x_j}\left[\left(\mu + \frac{\mu_t}{\sigma_\varepsilon}\right)\frac{\partial \varepsilon}{\partial x_j}\right] + C_{1\varepsilon}\frac{\varepsilon}{k}(P_k + C_{3\varepsilon}P_b) - C_{2\varepsilon}\rho\frac{\varepsilon^2}{k} + S_\varepsilon \qquad (3.8)$$

In equation (3.7) and (3.8) the "$\rho$" symbol is referring to density and "*the turbulent viscosity is modeled as:*

$$\mu_t = \rho C_\mu \frac{k^2}{\varepsilon} \qquad (3.9)$$

For further explanation of the equations (3.7) and (3.8) the equation of the modelled production term ($P_k$ in the k equation) is as follows:

$$P_k = -\mu_t S^2 \qquad (3.10)$$

Furthermore, the modulus of mean rate of stain tensor $S$ is as follows:

$$S = \sqrt{2S_{ij}S_{ij}} \qquad (3.11)$$

*The variables that are used in the equations (3.7), (3.8) and (3.9) are the following:*

$$C_\mu = 0.09 \quad \sigma_k = 1.00 \quad \sigma_\varepsilon = 1.30 \quad C_{1\varepsilon} = 1.44 \quad C_{2\varepsilon} = 1.92 \tag{3.12}$$

### 3.4.3. RNG k – ε turbulence model

The RNG k-e turbulence model derived from the theory of the Re-normalization group. The idea of continually removing the smallest scales of turbulence to a point where the remaining scales are resolvable with available computer capacities was formulated by the Yakhot et al [11]. As an aftermath, this model aims to modify the epsilon part of the model for different scales of motion though changes of the production term. For turbulent kinetic energy *k*, *the* equation is as follows:

For the dissipation rate *ε of the turbulent kinetic energy*, *the* equation is as follows:

$$\frac{\partial}{\partial t}(\rho\varepsilon) + \frac{\partial}{\partial x_j}(\rho\varepsilon u_j) = \frac{\partial}{\partial x_j}\left[\left(\mu + \frac{\mu_t}{\sigma_\varepsilon}\right)\frac{\partial \varepsilon}{\partial x_j}\right] + C_{1\varepsilon}\frac{\varepsilon}{k}P_k - C'_{2e}\frac{\varepsilon^2}{k} \tag{3.13}$$

The coefficient $C'_{2e}$ is given by:

$$C'_{2e} = C_{2e} + \frac{C_\mu \eta^3 (1-\frac{\eta}{\eta_0})}{1+\beta\eta^3} \tag{3.14}$$

*The variables that are used in the equations (3.13) and (3.14) are the following:*

$$C_\mu = 0.0845 \quad \sigma_k = 0.7194 \quad \sigma_\varepsilon = 0.7194 \quad C_{1\varepsilon} = 1.42$$

$$C_{2\varepsilon} = 1.68 \quad n_0 = 4.38 \quad \beta = 0.012 \tag{3.16}$$

Furthermore, RNG k-e model has shown very promising results in internal environment air simulations.

### 3.4.4. Chen – Kim k – ε turbulence model

Chen and Kim [12,13] have attributed some diffusive results of the standard k-ε model, to the nature of the dissipation rate which is highly empirical. Thus, they proposed an addition to the dissipation rate equation which was a second time scale of the production range of turbulence kinetic energy spectrum. As the

aftermath of this addition the energy transfer mechanism of the turbulence model responded to the mean strain more coherently. Furthermore, one additional term and a modeling constant was added to the standard k-ε model, based on the experimental data of homogeneous turbulence decay. As a result the additions to the standard model are as follows:

The variables of the empirical values are as follows:

$$\sigma_k = 0.75 \quad \sigma_\varepsilon = 1.15 \quad C_{1\varepsilon} = 1.15 \quad C_{2\varepsilon} = 1.9 \quad C_{3\varepsilon} = 0.25 \tag{3.17}$$

In the dissipation rate ε of the turbulent kinetic energy, including the second time scale $\frac{k}{P_k}$, the volumetric source term takes the form:

$$S_\varepsilon = \frac{\rho F_1 C_{3\varepsilon} P_k^2}{k} \tag{3.18}$$

$F_1$: Lam and Bremhorst's [14] damping function

### 3.5. Boundary conditions

In this section the initial and boundary condition that are defining the problem will be discussed.

#### 3.5.1. Velocity inlet

In this problem there are two types of velocity inlet in both designs. All distances of the objects are given from the center of each object. The air-condition air is introduced in the supermarket as inlets having a constant velocity of 0.5 m/s. In the first design six units placed at 7.5 meters height. Three are placed in the plane Ymin and the other three in Ymax at 25 m. The placement at X axis is 4.5, 11 and 17 m and is the same for the three at the opposite side of the room. In the second design we have 2 units in the same side of the room, placed at 2.5 m in the Z axis and at 3 and 8.5 m in the X axis respectively. The temperature of the cool stream is equal to 14 $^{o}$C in order to convey the thermal load of the building. The second inlet was selected to simulate the mouth and nose of a virus contaminated person in a state of sneezing and coughing. Furthermore, the inlet that describe the mouth and nose has dimensions X=10 cm and Y=20 cm in the first design and X=5 cm and Y=8 cm in the second design. The person releases a spray of virus contaminated droplets (C=1, concentration of COVID-19) at a speed of 4.5 m/s.

The temperature at this inlet is 40°C. In the design 1, there is also a healthy person, whose body temperature is 36,6 °C.

### 3.5.2. Outlet

Design 1 has two doors and four air-extraction vents that were used as outlets. Design 2 has one doors that is used as outlet. The temperature at which the flow exits the building is 24 °C. Moreover, it is assumed that the outlet pressure is equal to the external atmospheric pressure. The air-extraction vents are placed on the ceiling of the supermarket.

### 3.5.3. Walls

All the walls of the building were defined as adiabatic walls. Furthermore, all the countertops and racks are considered also as adiabatic blocks (25 °C).

### 3.5.4. Human Model

The human model is 1.75 m tall. The model was selected to be as simple as possible regarding its geometry. Its boundary condition is set as an adiabatic body. Furthermore, the body acts as a blockage of concentration, thus the concentration inside is 0%.

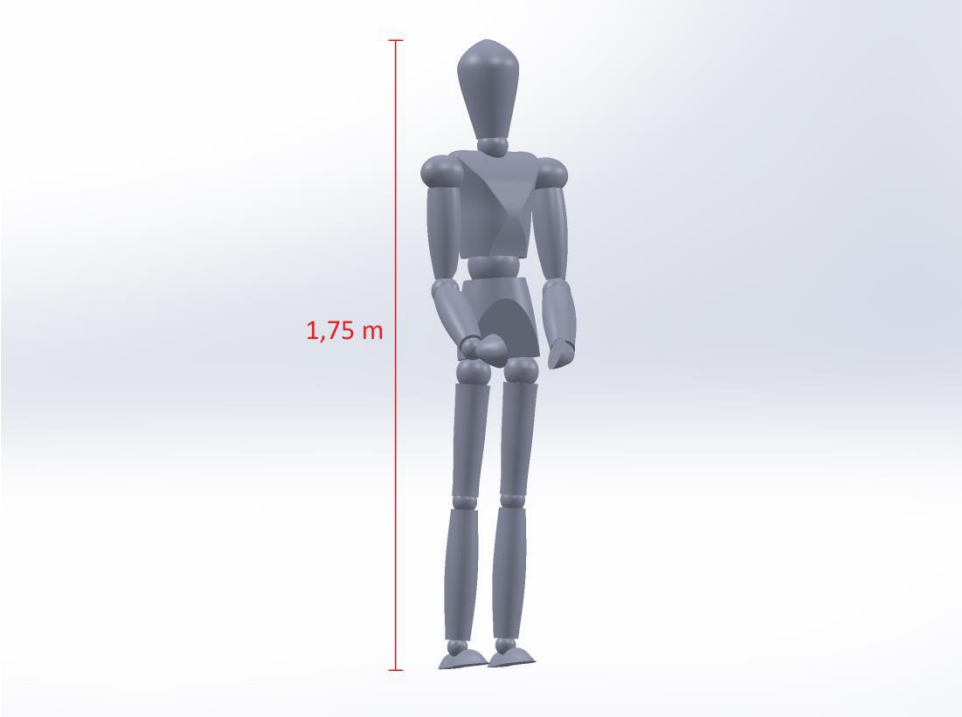


*Figure 4 – Human model CAD design*

### 3.6. Computational procedure

The default linear equation solver for each finite-volume equation was used for the coarse grid and first stages of this research, that is a form of Stone's [14] strongly implicit solver. Which does not use a pre-conditioner. As it noted in the Phoenics documentation "TR 006" [15] if the parallel solver option is enabled, as it was in the present's case finer grids, the Stone's solver is replaced by a parallel version of the CGRS [16] solver. The mentioned solvers are included in the CFD package of Phoenics 2020 and are used without being changed.

### 3.7. CPU time requirements

The CPU time required for the optimum grids of the problem considered to obtain full convergence was obtained within 10-14 hours for the 1.357.752 cells grid of design 2, depending on the different scenarios and the turbulence model used. Computations were performed on a Windows 7 Server (Intel Xeon 2650 v2 8 core 16 threads, 2.60 GHz CPU and 32GB of RAM).

# 4. Results

## 4.1. Spatial discretization

For the numerical solution, a multi-block non-uniform structured grid for each of the two cases is used. The grid is locally refined around the critical area of the two people. The grid after the refinement around the human model and the mouth and nose described in the form of Figure 4.

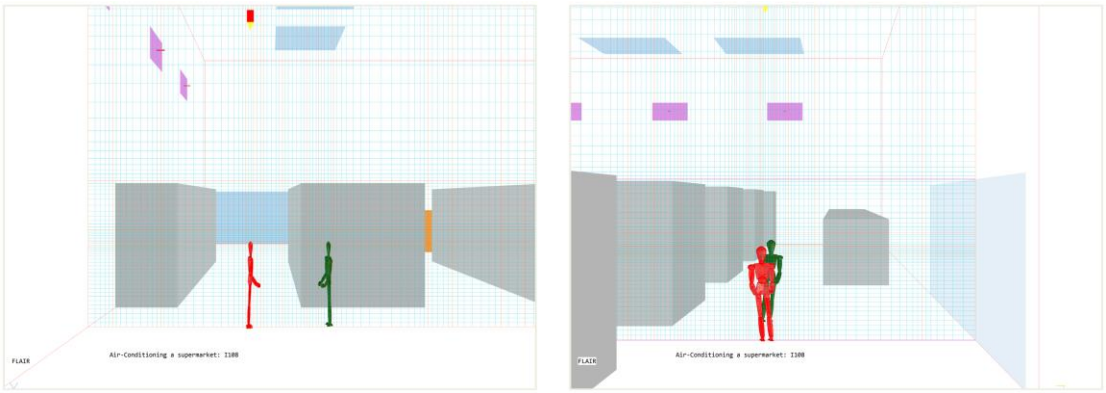

*Figure 5* – Depiction of the problem's computational grid and the local refinement around the human model (Design 1)

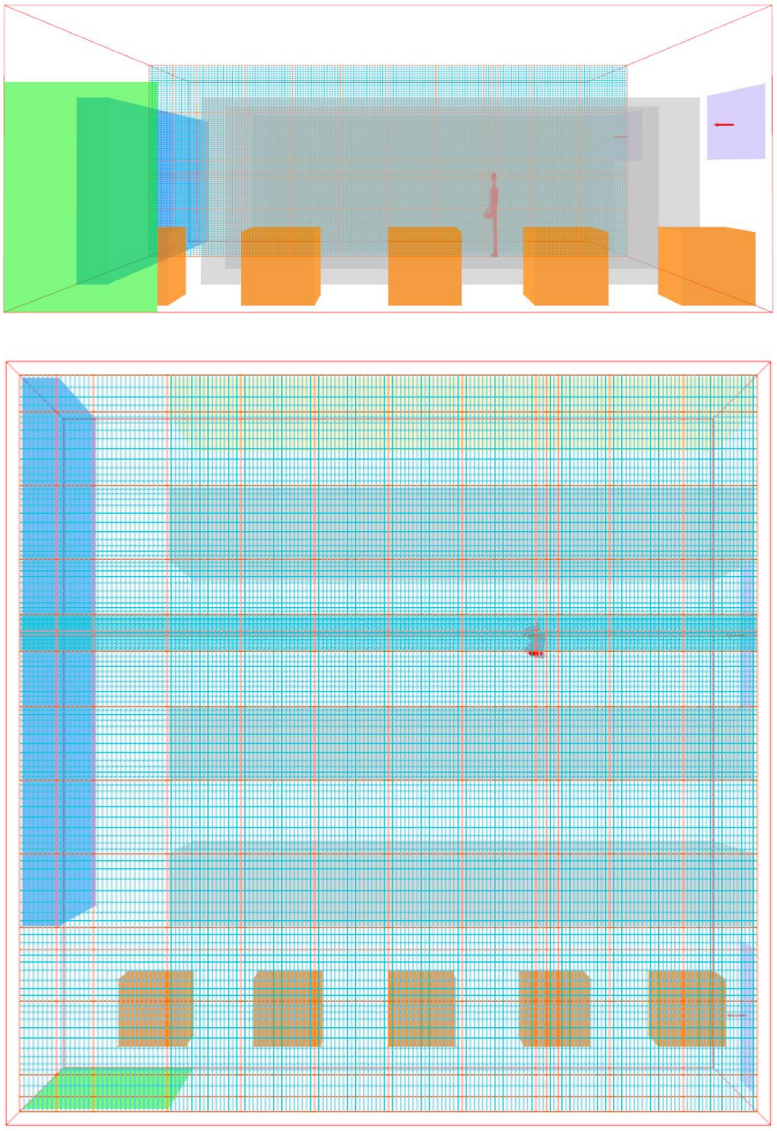

*Figure 6 - Depiction of the problem's computational grid and the local refinement around the human model (Design 2)*

### 4.2. Results of different turbulence models

#### 4.2.1. Design 1

In Figure 6, the numerical results obtained by both turbulence models, are presented, for the case there is an open window in the domain.

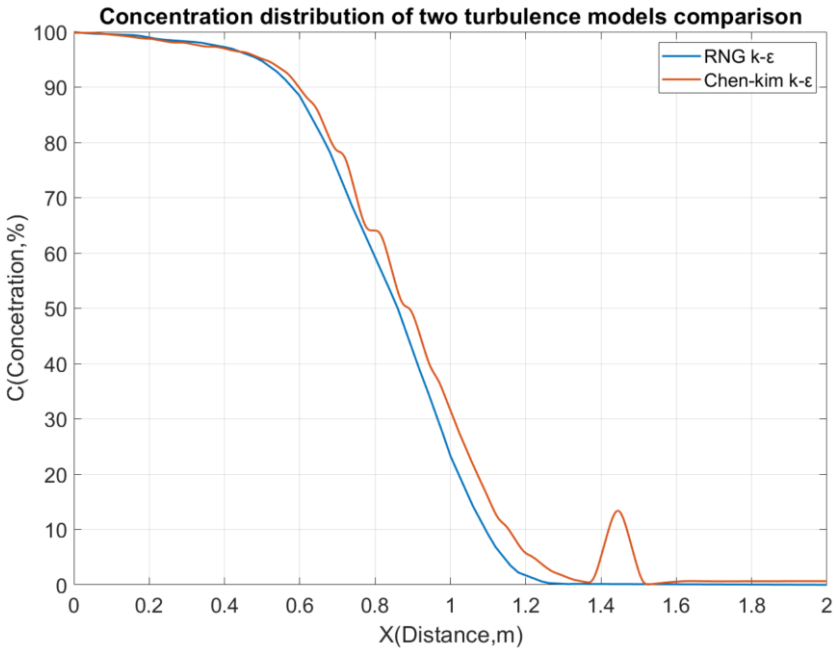


*Figure 7 - Concentration distribution of the two turbulence models (Chen-kim k-e and RNG k-e).*

### 4.2.2. Design 2

As already mentioned, in this case, two different turbulence models were used, in order to perform the calculations; the Chen-Kim k-ε turbulence model and the k-ω SST turbulence model. In this section, the results acquired by both of these models, are presented.

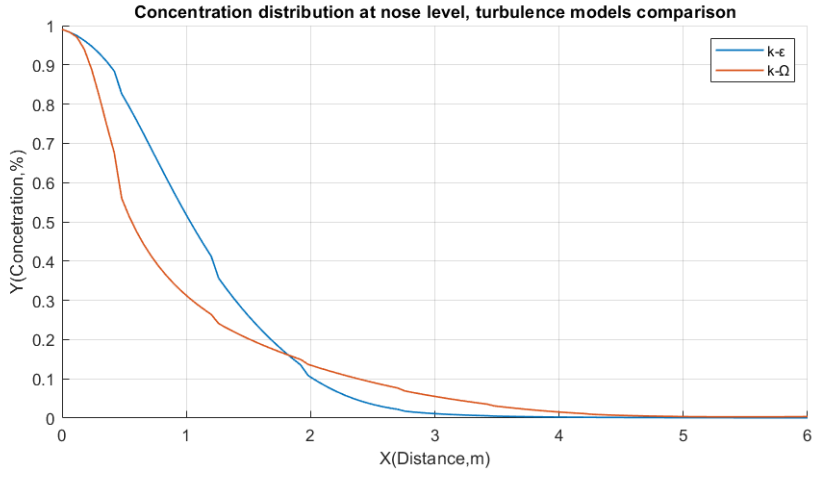

*Figure 8 - Comparison of the results, acquired by the two turbulence models. The air-conditioning inlet velocity is equal to 0.8 m/s, for this comparison.*

### 4.3. Grid independency study

#### 4.3.1. Design 1

Grid independency is also tested, by repeating the simulation for a gradually increased grid-cell density. Three grid sizes are tested: the first consisted of 1.301.984 cells, the second consisted of 2.213.120 cells and the third consisted of 2.277.960 cells; the optimum spatial discretization is that of 2.213.190 cells. The used grids, as well as the optimum grid for the problem are presented in Figures 8 and 9.

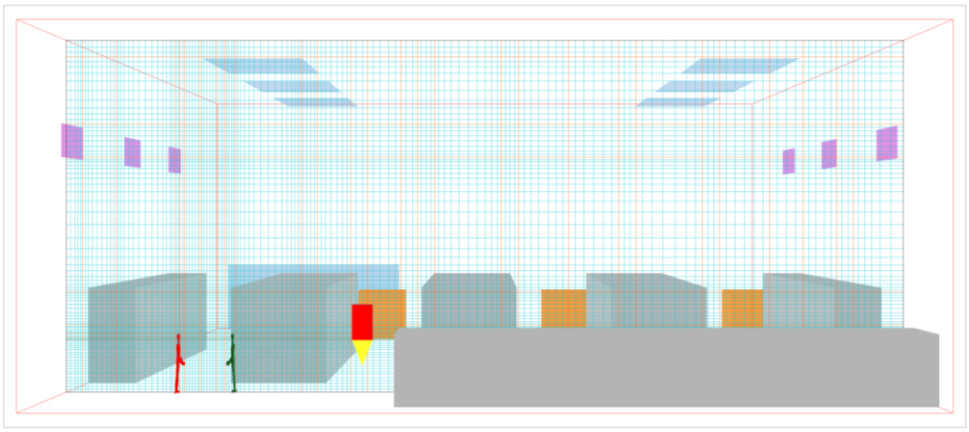

(a)

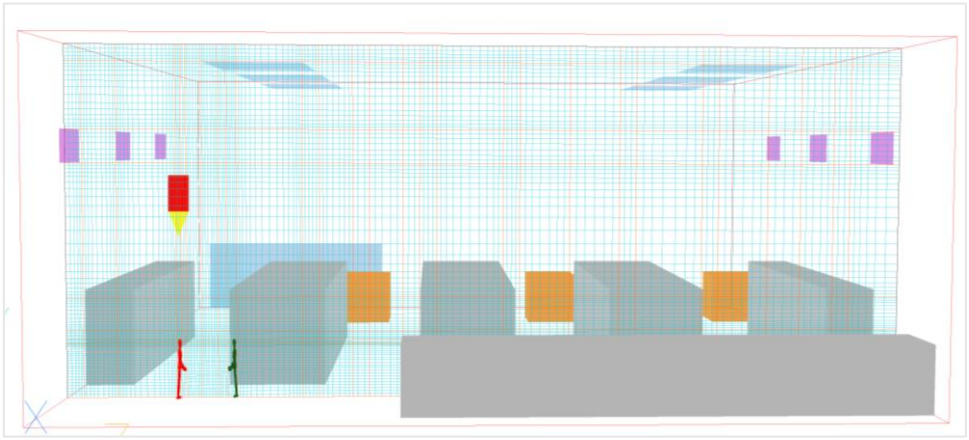

(b)

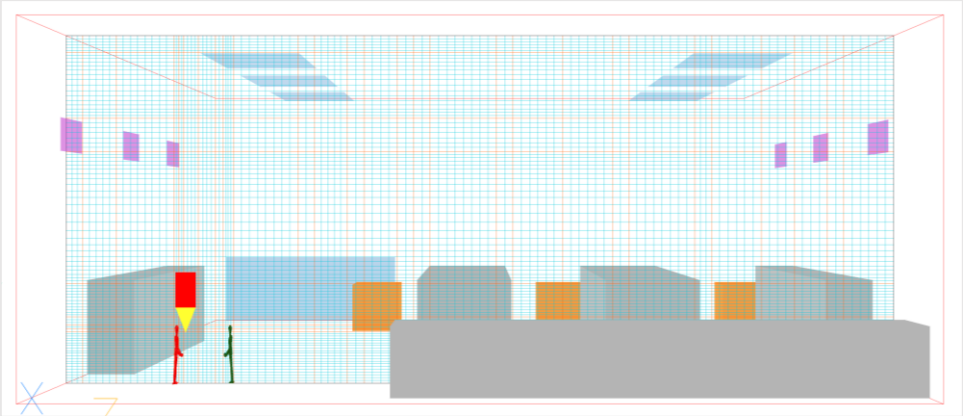

(c)

*Figure 9 - Depiction of the three different grids that are tested, the first consisting of 1.301.984 cells (a), the second of 2.213.120 cells (b) and the third of 2.277.960 cells (c).*

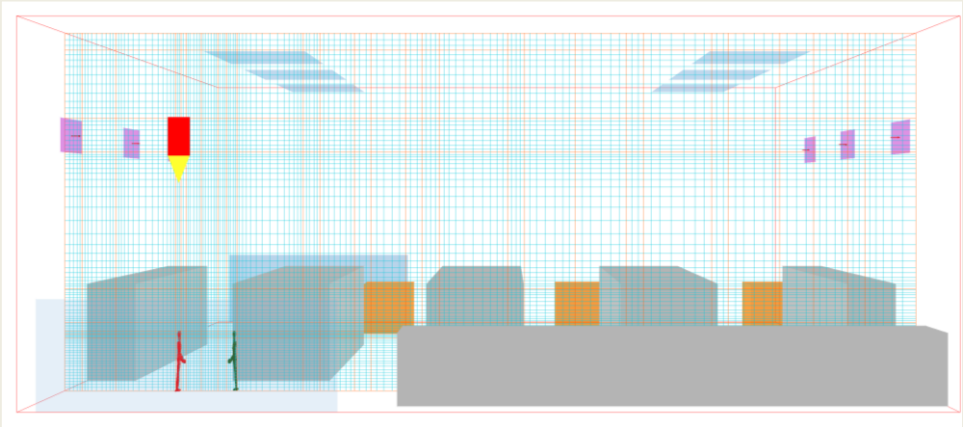

(a)

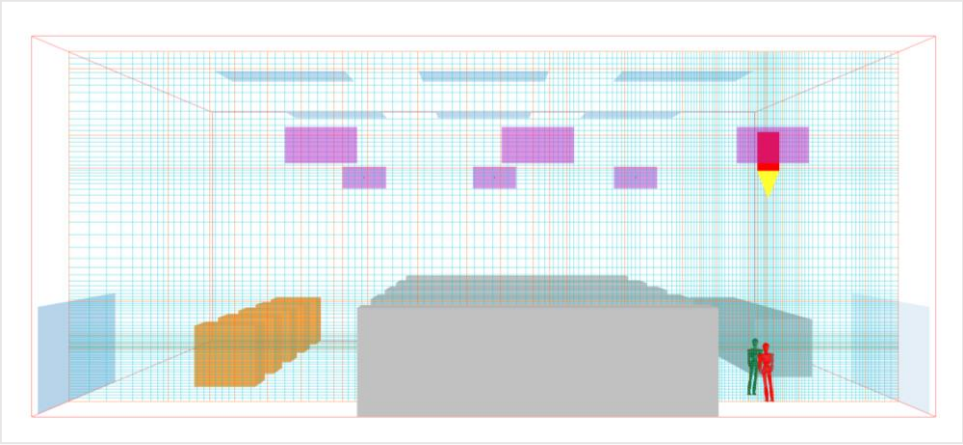

(b)

Figure 10 - Optimum spatial discretization: (a) Y-Plane view and (b) X-Plane view

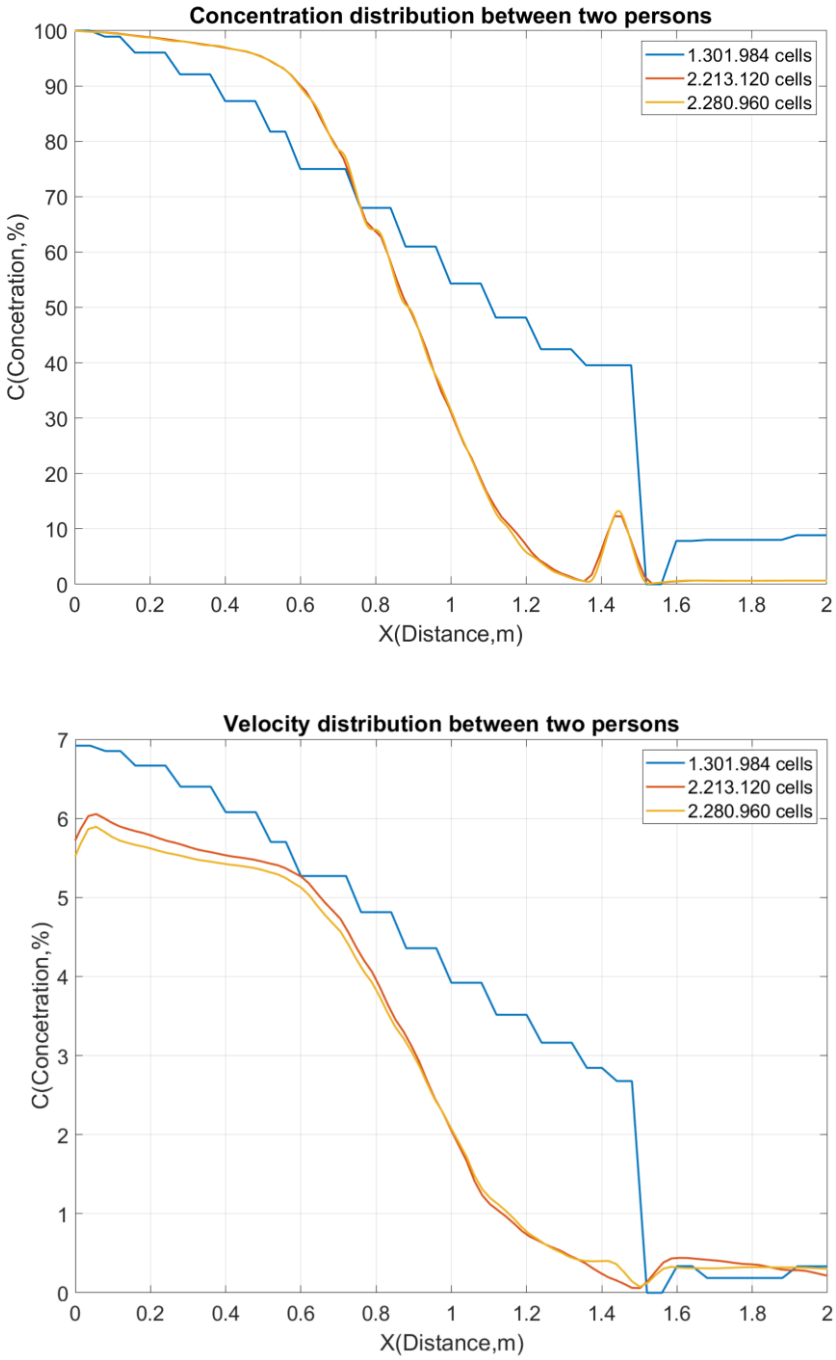


*Figure 11 - Horizontal distribution of concentration in height z=1.60m between the two human models, 1.301.984 cells purple, 2.213.120 cells green and 2.277.960 cells blue (top) concentration (bottom) velocity*

### 4.3.2. Design 2

Apart from the standard calculations, grid independency is also tested, by repeating the simulation for a gradually increased grid-cell density. Three

different types of grids are tested, of which the coars e one consists of 770.000 cells, the medium one consists of 1.357.752 cells and the fine one consists of 2.047.000 cells.

For the case of a closed window in the computational domain, the virus concentration distribution, at the person's nose height, for the three computational grids, can be seen in Figure 13.

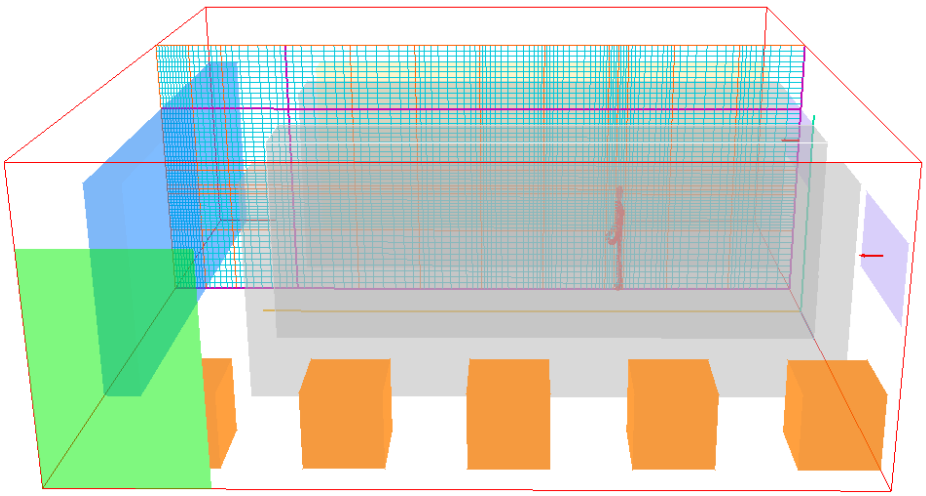

a)

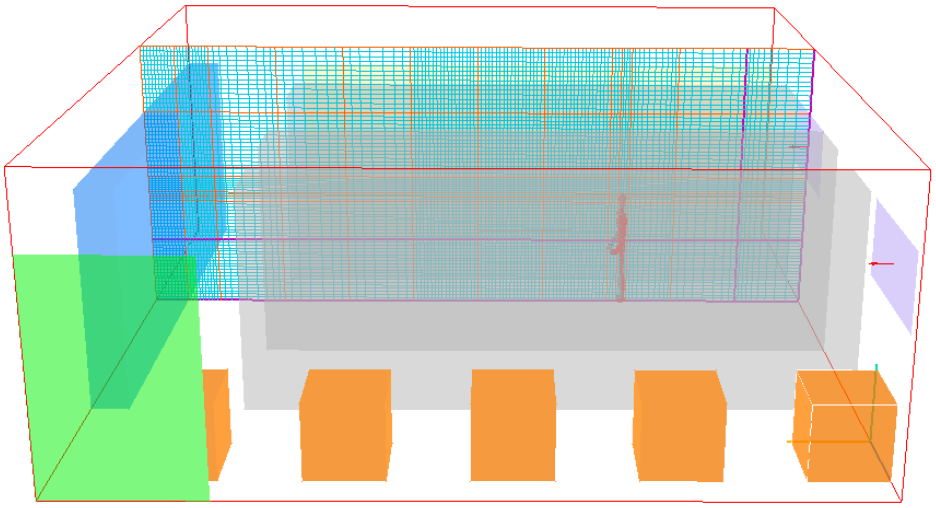

b)

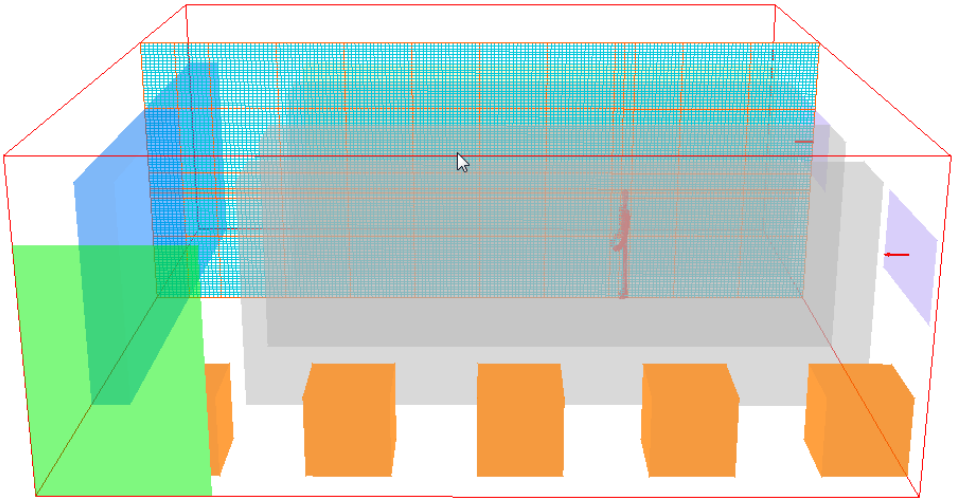

*c)*

*Figure 12* - Depiction of the three different grids that are tested, the first consisting of 770.000 cells (a), the second of 1.357.752 cells (b) and the third of 2.047.000 cells (c)

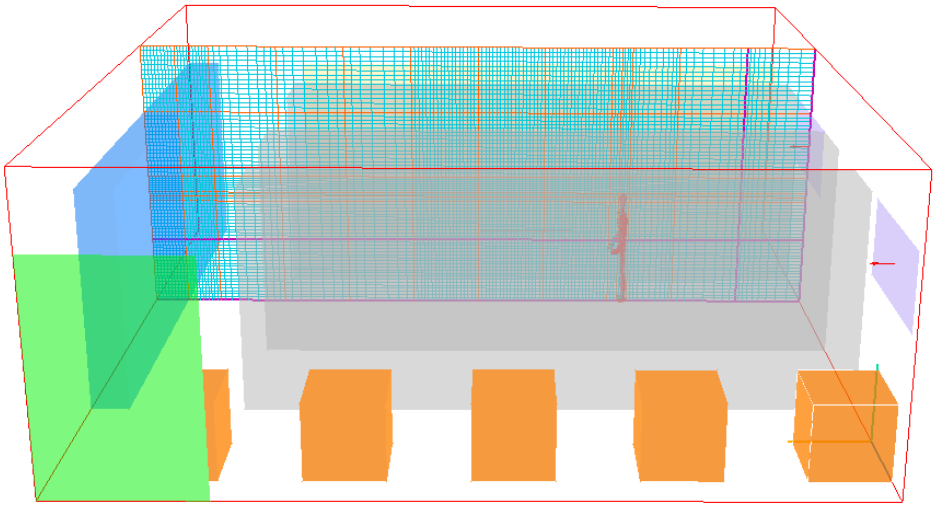

*a)*

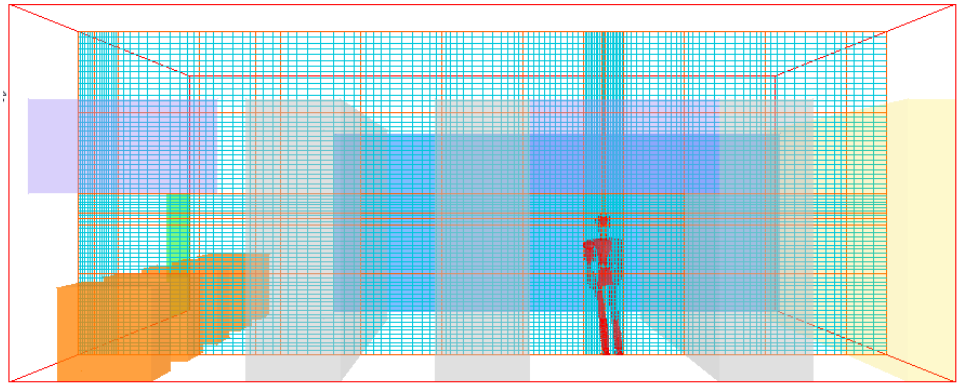

*b)*

*Figure 13- Optimum spatial discretization: (a) Y-Plane view and (b) X-Plane view*

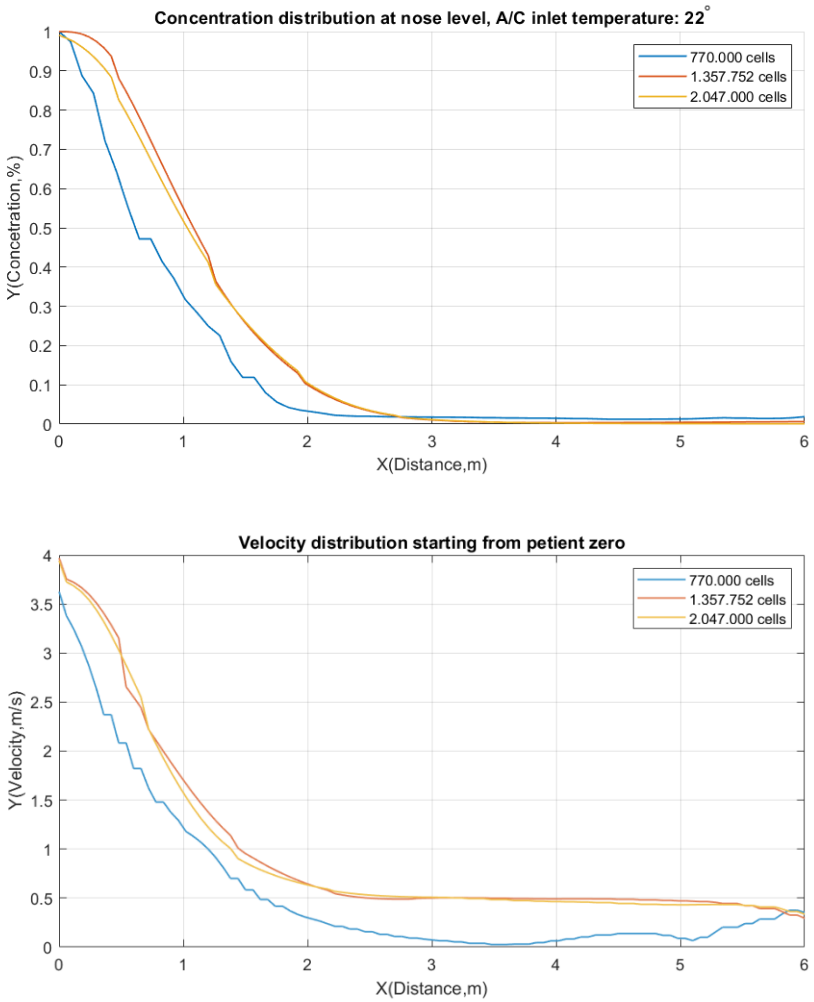


*Figure 14 - Horizontal distribution of concentration in height z=1.60m between the two human models 770.00 cells purple, 1.357.752 cells green and 2.047.000 cells blue (top) Concertation (bottom) Velocity*

As is seen in Figure 14, the coarse grid's results for the concentration distribution differ significantly from the results obtained by the other two types of computational grids. The medium and fine grids, however, yield results of high accordance, which display only a slight divergence at a distance of up to approximately 1.2 meters.

## 4.4. Parametric study results

### 4.4.1. Design 1

Three different scenarios have been conducted. In the first, the A/C units have been placed in 8 m above the floor and the temperature of the air in the A/C has been set to 14 ℃, in the height in which the A/C units placed change to 4 m and in the temperature of the units was changed to 18 ℃.

*Table 2 – Attributes of the cases*

| Attributes/Case No. | Case 1 | Case 2 | Case 3 |
|---|---|---|---|
| Height of A/C unit (m) | 8 | 4 | 4 |
| Temperature of the air | 14 | 14 | 18 |

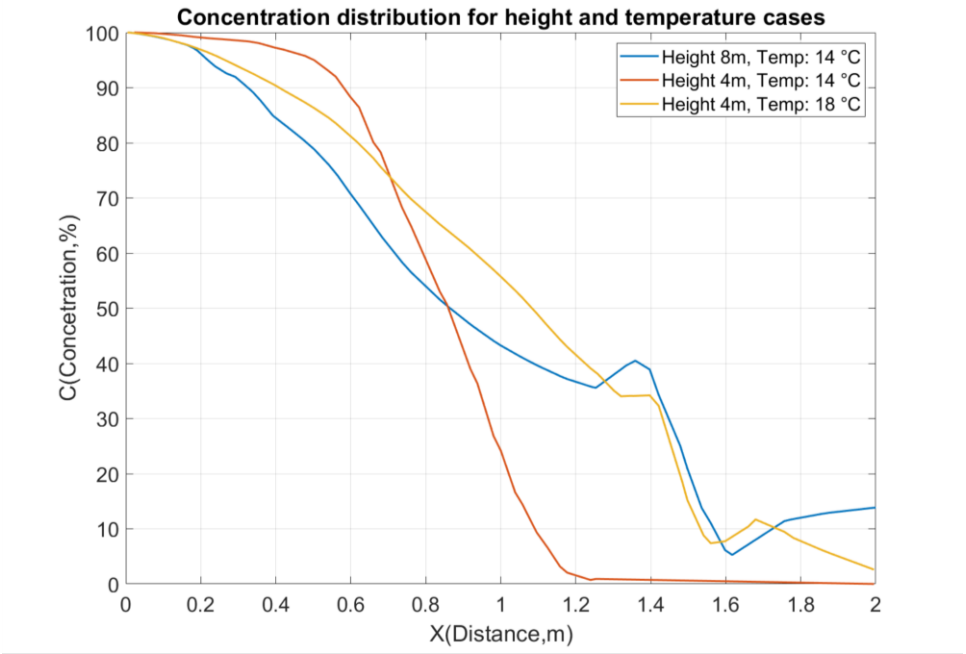


*Figure 15 - Concertation distribution of the three cases*

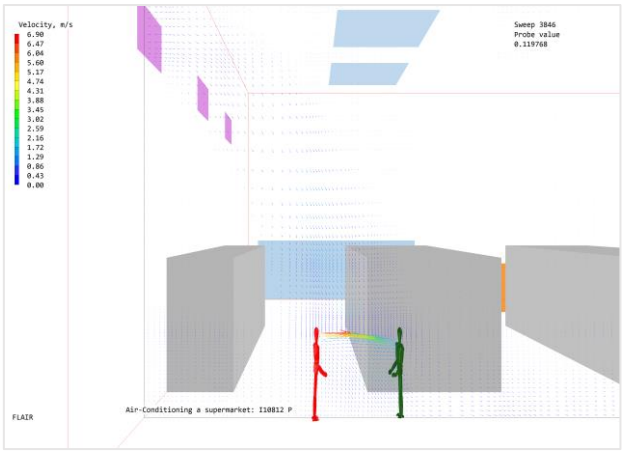

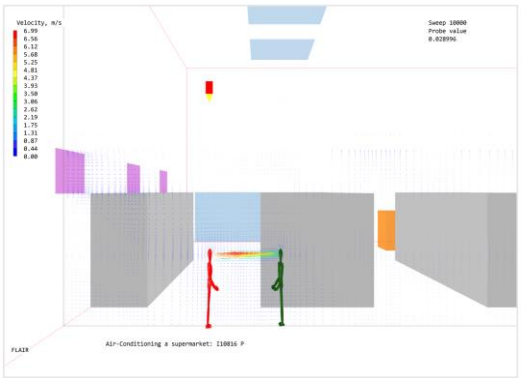

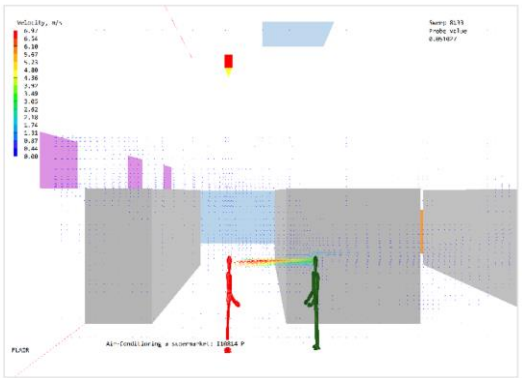

*Figure 16 - Vectors of velocity in Y-Plane view, (top) Case 1 A/C units at 8 m height and 14 °C, (left) Case 2 A/C units at 4 m height and 14 °C, (right) Case 3 A/C units at 4 m height and 18 °C*

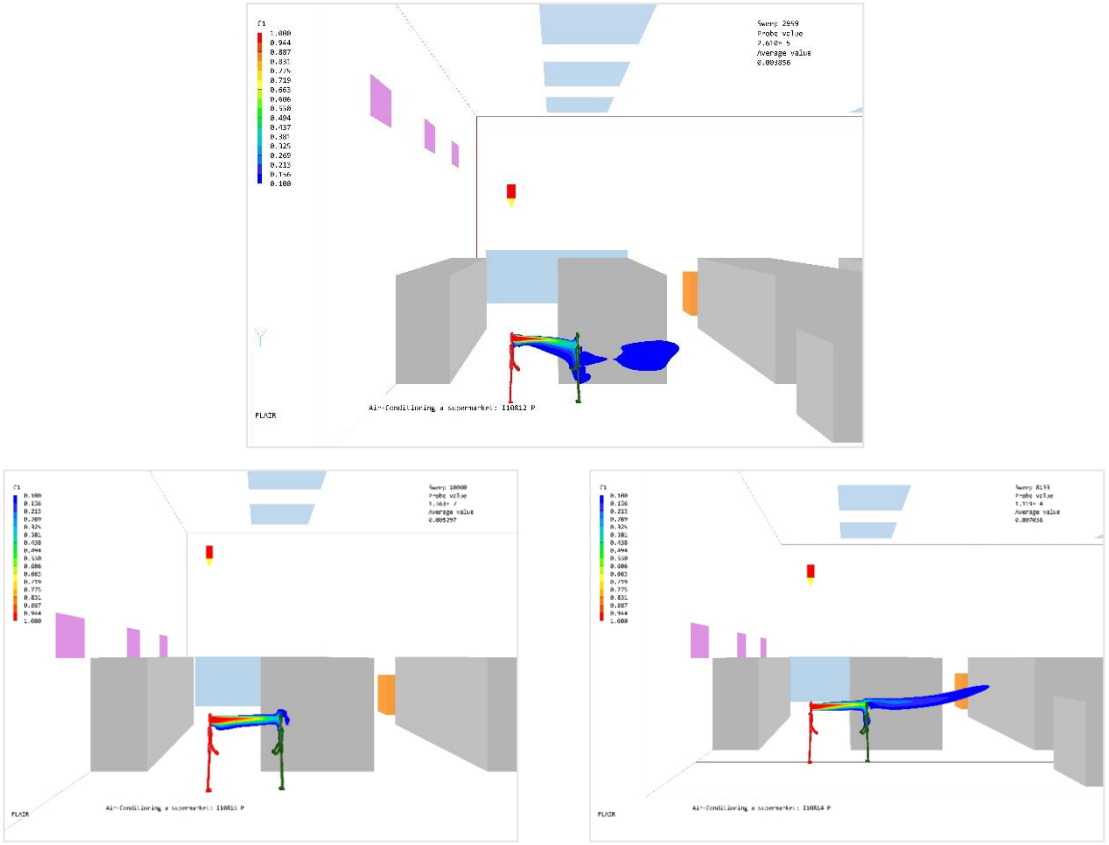

*Figure 17 - Contour of concentration in Y-Plane view, (top) Case 1 A/C units at 8 m height and 14 °C, (left) Case 2 A/C units at 4 m height and 14 °C, (right) Case 3 A/C units at 4 m height and 18 °C*

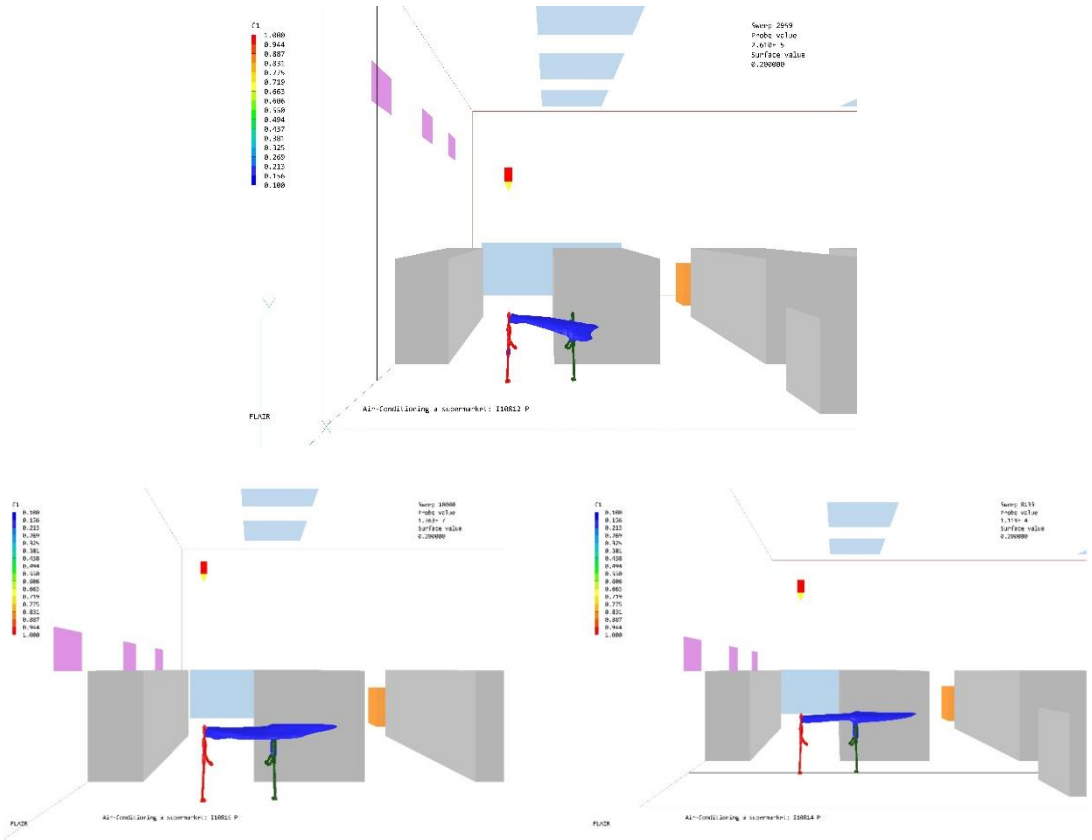

*Figure 18 - Iso-surface contours of concentration in Y-Plane view, (top) Case 1 A/C units at 8 m height and 14 °C, (left) Case 2 A/C units at 4 m height and 14 °C, (right) Case 3 A/C units at 4 m height and 18 °C*

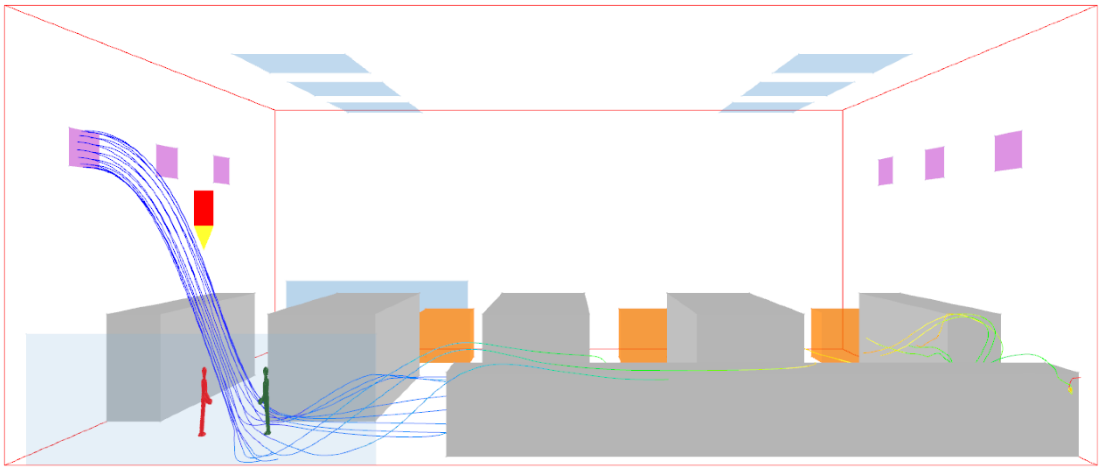

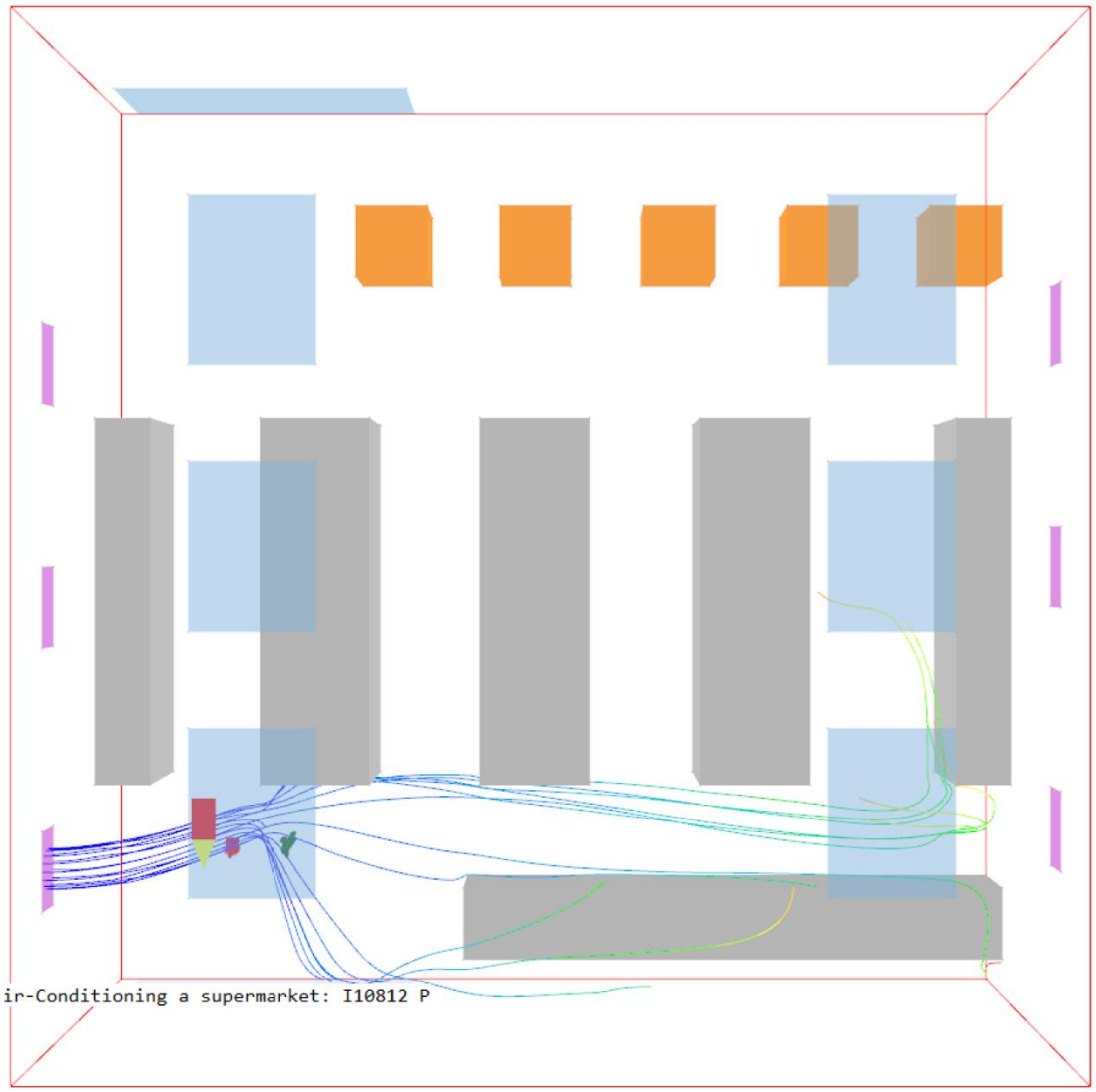


*Figure 19 - Streamlines units at 8 m height and 14 °C*

### 4.4.2. Design 2

For the case in which the air-conditioning air's temperature is higher and equal to 18 °C (in order to ensure that the warmer air does not allow contaminated particles to get entrained towards the floor), the concentration distribution in the X-direction was studied for 3 different cases, which are presented in *Table 1*. The height, in which the air-conditioning units are placed, is equal to 4 m, in all cases.

*Table 3* - Attributes of the 3 cases studied.

| **Case No.** | **Case 1** | **Case 2** | **Case 3** |
|---|---|---|---|
| **Air-conditioning inlet velocity (m/s)** | 0.2 | 0.4 | 0.8 |

In this case study, only one human model was taken into account, so as to examine how far the virus-containing particles are transmitted. The reason for this is that the existence of a second human model complicates this simulation, due to the fact that it acts as a blockage, thus distorting the concentration's distribution.

The results for the Chen-Kim k-ε turbulence model are presented in *Figure 1*.

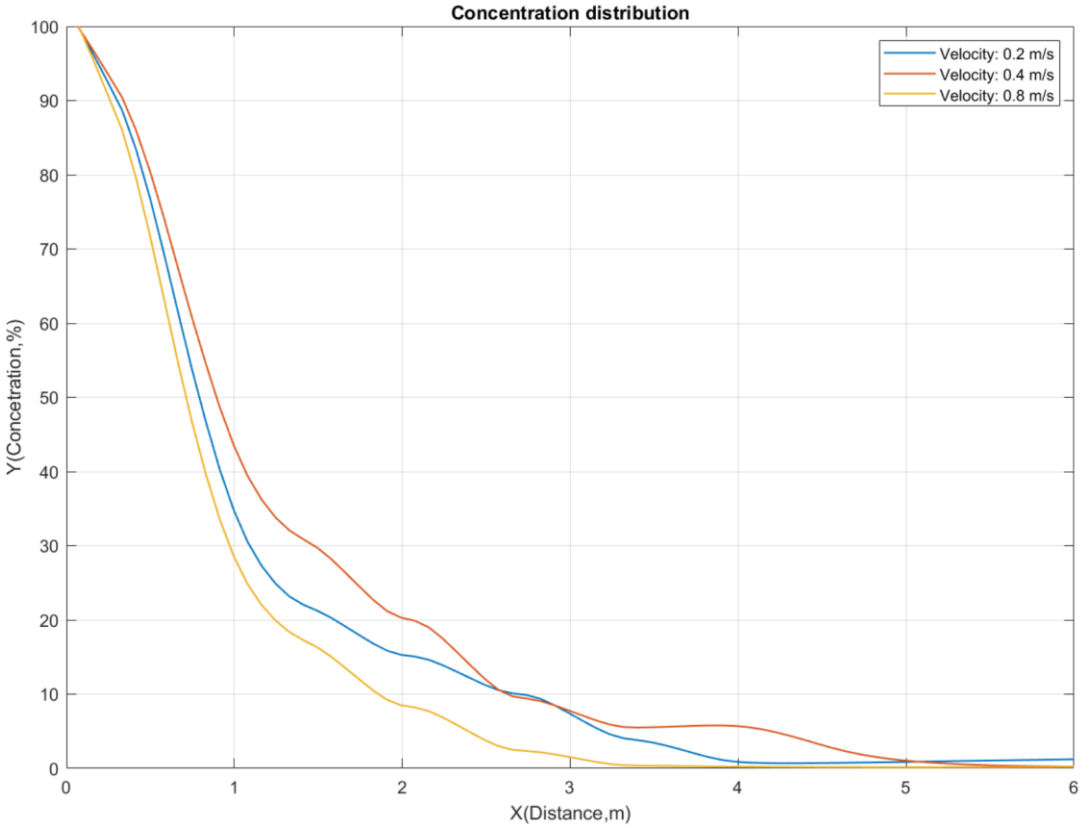


*Figure 20 - Depiction of the virus concentration distribution, for the three different cases. The blue line represents an air inlet velocity of 0.2 m/s, the red line represents an air inlet velocity of 0.4 m/s and the green line represents an air inlet velocity of 0.8 m/s.*

## 4.5. Analysis

### 4.5.1. Design 1

From *Figure 1*, it becomes clear that the virus concentration is quite high, even at a distance of 4 meters from the contaminated person, at least for two of the three air inlet velocities (approximately 5% for an inlet velocity of 0.2 m/s and approximately 10% for an inlet velocity of 0.8 m/s).

It has been experimentally found that a healthy person has a 17% probability of getting infected at a distance of 1.5 meters from a contaminated person. This probability drops to just 3%, at a distance of 3 meters. If one assumes that the probability of someone getting infected by the virus is proportional to the concertation of the virus, it follows that this concentration should be equal to 17% at a distance of 1.5 meters and 3% at a distance of 3 meters.

By the results achieved in this particular case study, it is noticed that the virus concentrations for the three different inlet velocities were calculated as follows:

- Inlet velocity of 0.2 m/s: approximately 28.1% at 1.5 m and 10.9% at 3 m
- Inlet velocity of 0.4 m/s: approximately 19.6% at 1.5 m and 0.7% at 3 m
- Inlet velocity of 0.8 m/s: approximately 30.4% at 1.5 m and 12.8% at 3 m

Thus, an inlet velocity of 0.4 m/s is more favorable for the quicker drop of the virus concentration, while also, seemingly, being in compliance with the experimental observations.

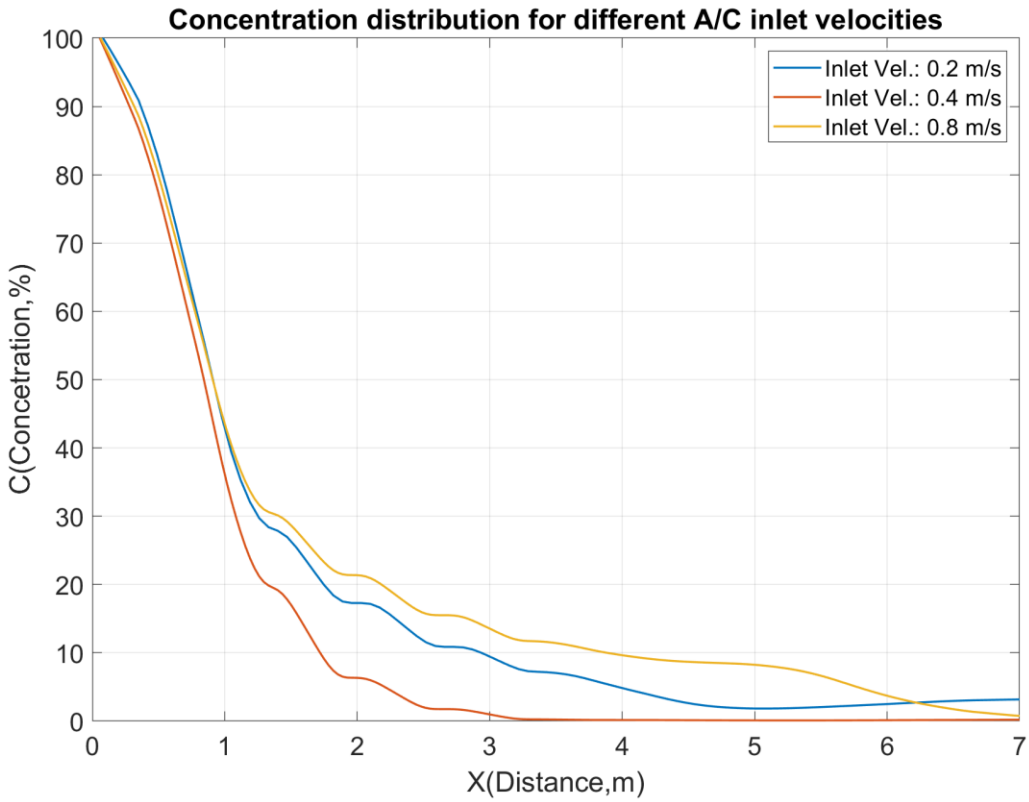


*Figure 21 - Depiction of the virus concentration distribution, for the three different cases and a distance up to 7 meters.*

In order to further investigate the three cases, the concentration's distribution was also plotted up to a distance of 7 meters. The results are shown in Figure 1. For an air inlet velocity of 0.2 m/s, the lowest virus concentration value is marked at a distance of approximately 5 meters and is equal to 1.8%, while for an inlet velocity of 0.8 meters, this value is equal to 0.85% and is marked at a distance of 6.9 meters.

It is proven once again that the velocity of 0.4 m/s is the most advantageous, since it provides a lowest concentration value of 0.084% at a distance of 5.25 meters.

### Calculation of the virus concentration distribution, for different air temperatures

The concentration distribution of the virus was also calculated, for different cases of air-conditioning air temperatures, in order to comprehend the effect of the air

temperature on the way that the contaminated particles get transmitted throughout a portion of the domain.

More specifically, two cases were examined; in the first one, the air temperature is set equal to 18 $^{o}$C, while, in the second, it is set equal to 20 $^{o}$C. The distance between the air-conditioning units and the floor remains equal to 4 meters and the inlet velocity of the air is 0.4 m/s.

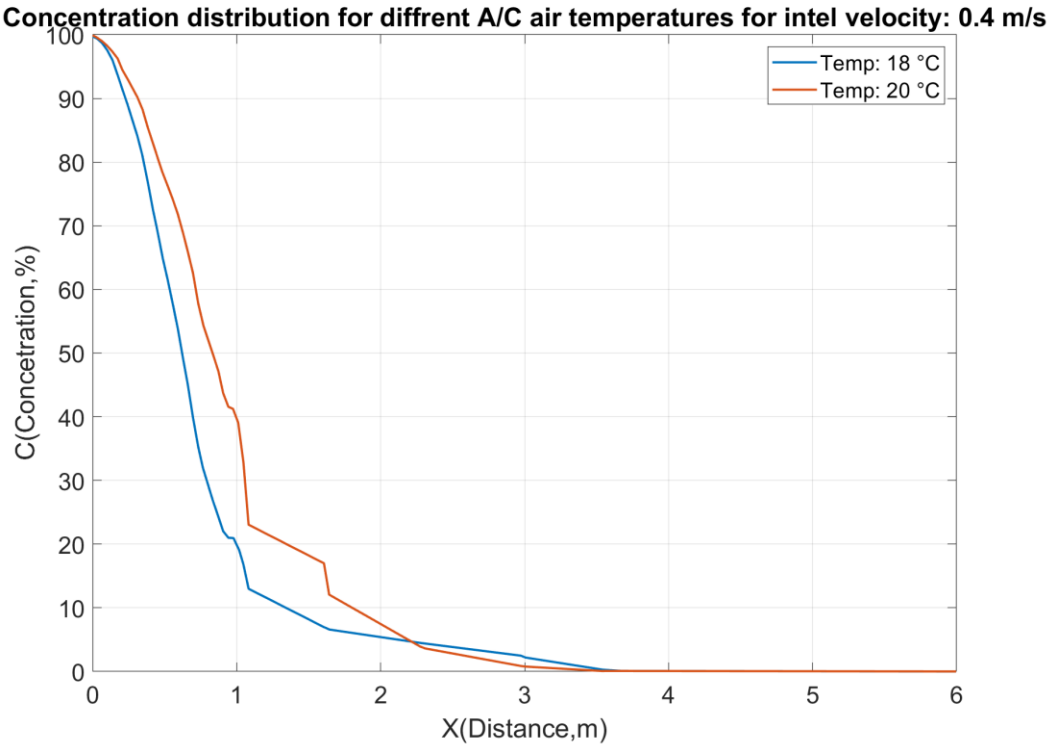


*Figure 22 - Depiction of the virus concentration, for the two different cases. The blue line represents an air temperature of 18 $^{o}$C, while the red line represents an air temperature of 20 $^{o}$C.*

The results for the Chen-Kim k-ε turbulence model are presented in *Figure 21*.

### 4.5.2. Design 2

In the case of a computational domain with closed windows, the effect that the alteration of air-conditioning inlet velocity has on the concentration distribution, is also studied. First, in Figure 22, the concentration distribution in case of the absence of air-conditioning is presented, while, in Figure 23, the concentration

distribution for three different air-conditioning inlet velocities is presented. The results regard the k-ω turbulence model.

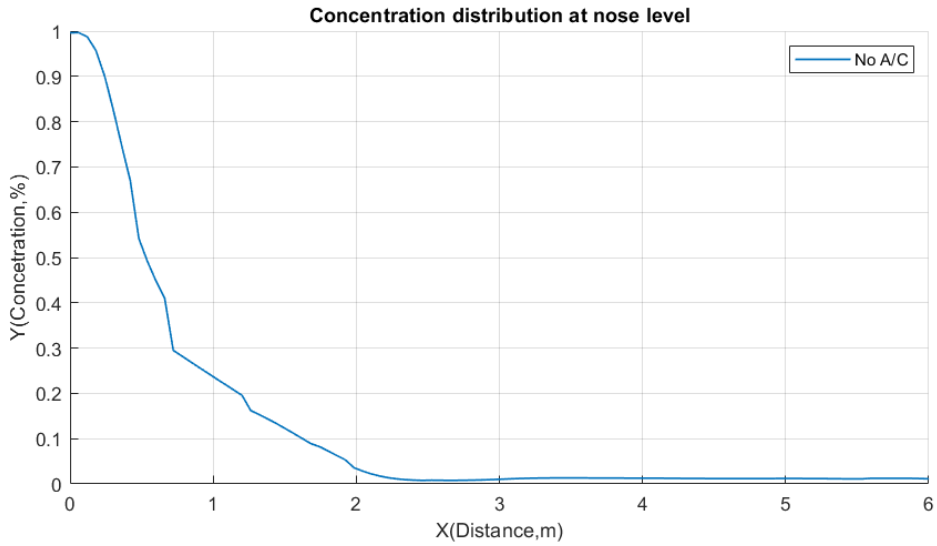


*Figure 23 - The virus concentration distribution, in case there is no air-conditioning.*

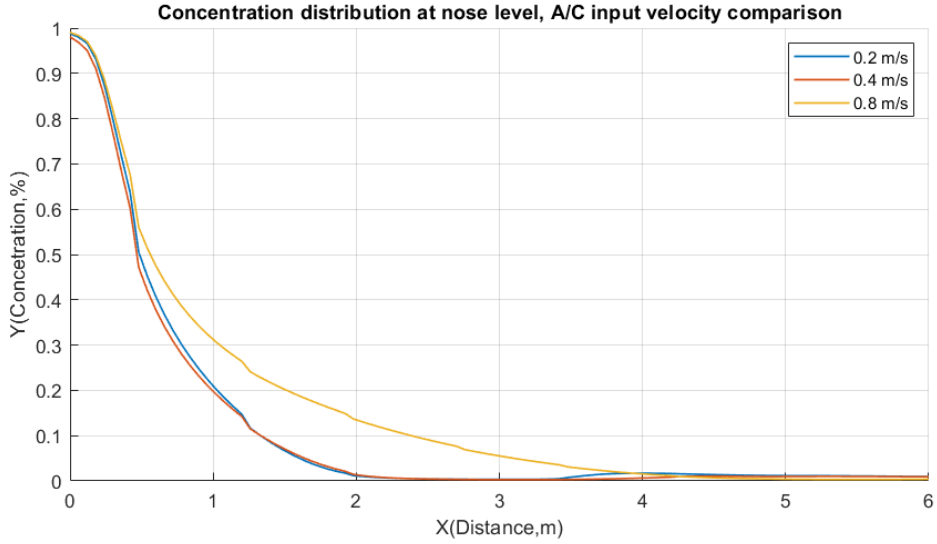


*Figure 24 - The virus concentration distribution, for three different air-conditioning inlet velocities, namely 0.2 m/s (mild air-conditioning), 0.4 m/s (moderate air-conditioning) and 0.8 m/s (intense air-conditioning).*

As expected, for lower air-conditioning inlet velocities (or in the case of absent air-conditioning), the virus does not get transmitted via a big distance, and its concentration diminishes in a faster rate, whereas, for an air-conditioning inlet

velocity of 0.8 m/s, the virus gets entrained further away, leading to significantly higher concentrations, in the distance range of approximately 0.8 meters to 3.5 meters. This can also be seen in Figures 24 and 25.

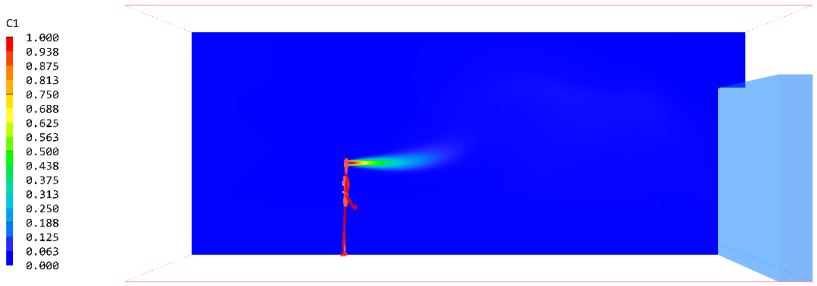


*Figure 25 - Virus concentration contours (no air-conditioning).*

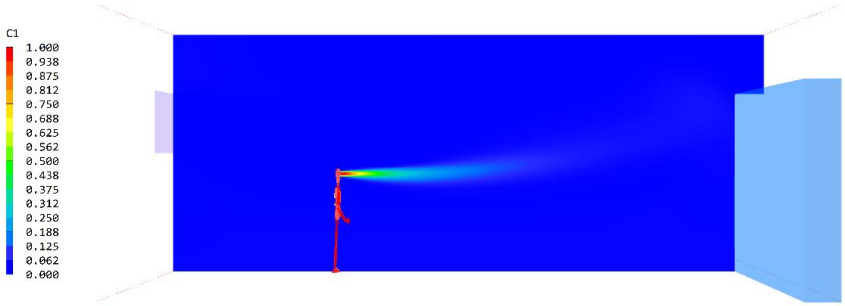


*Figure 26 - Virus concentration contours (air-conditioning with inlet velocity of 0.8 m/s).*

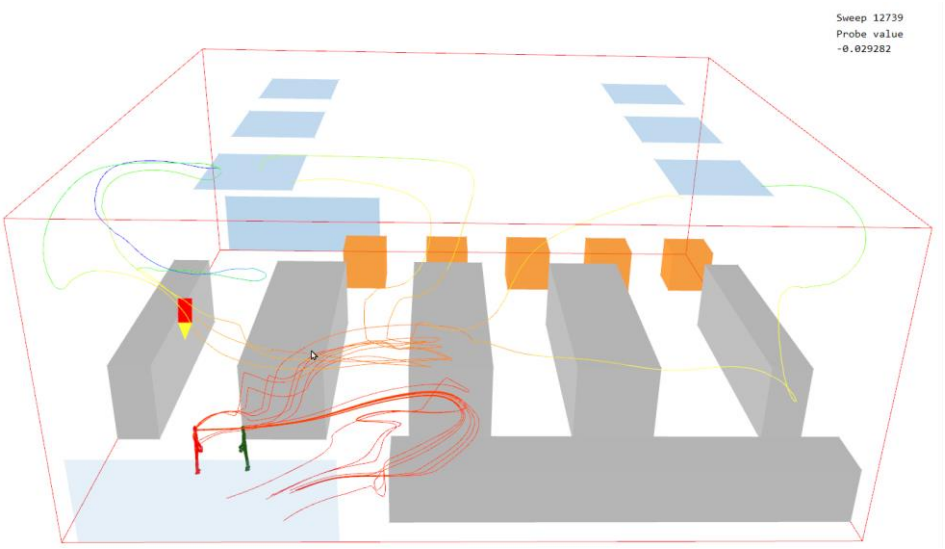


*Figure 27 – Streamlines staring from the mouth (No A/C)*

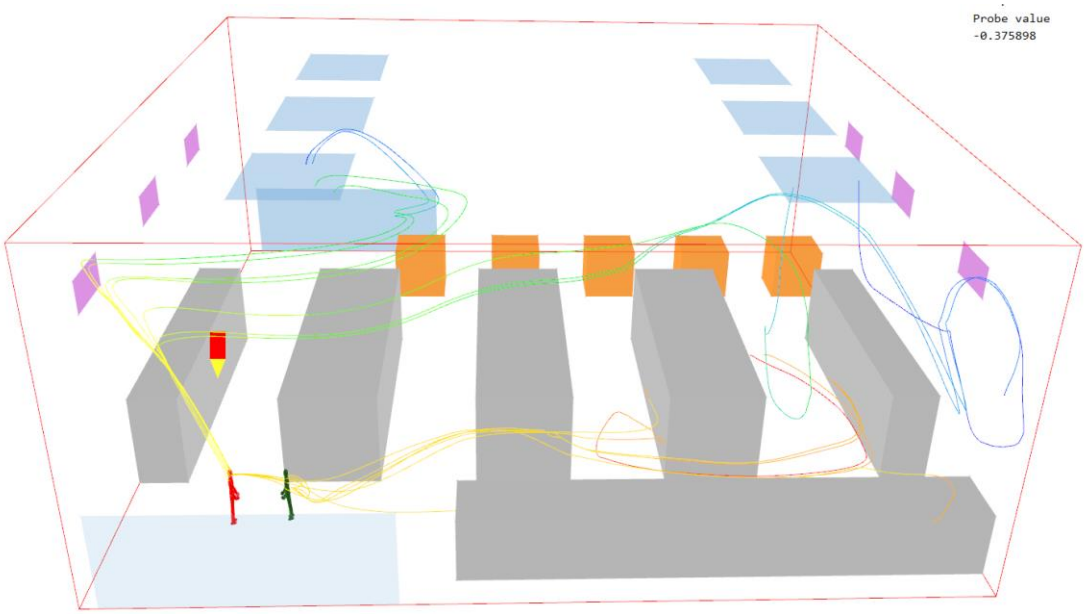


*Figure 28 – Streamlines starting from the A/C unit (A/C 0.8 m/s)*

### 4.5.3. Asymptomatic patient study at model 2

In design 2 an additional case did perform. The aim of this case was to point out the concentration in the room which contains an asymptotic patient. In the given case the inlet's velocity was set to a significant lower value of 0.8 m/s. This value is serving the purpose to simulate the average value of nasal breathing [17].

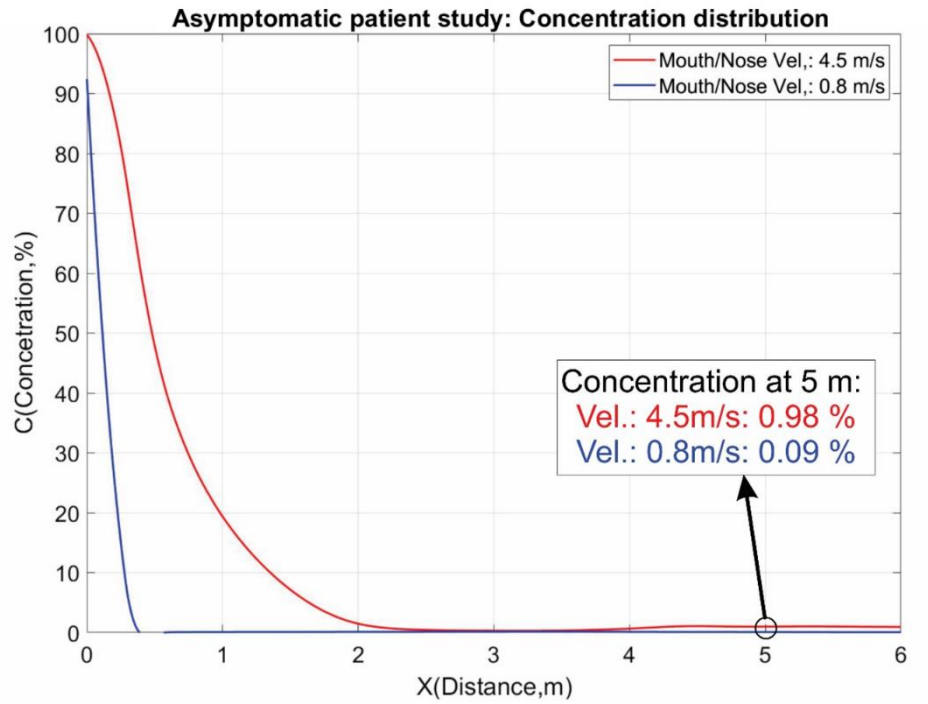


*Figure 29 – Asymptotic patient study concentration distribution*

The previous plot is depicted the contrast between two simulation of an average A/C inlet speed: the first simulation (red line) is as the previous runs, which contain an inlet of 4.5 m/s (sneezing). On other hand the second simulation (blue line) has the speed of a person that is breathing. In 5 m a small concertation of 0.09 is still present despite the greater distance from the inlet and the smaller velocity.

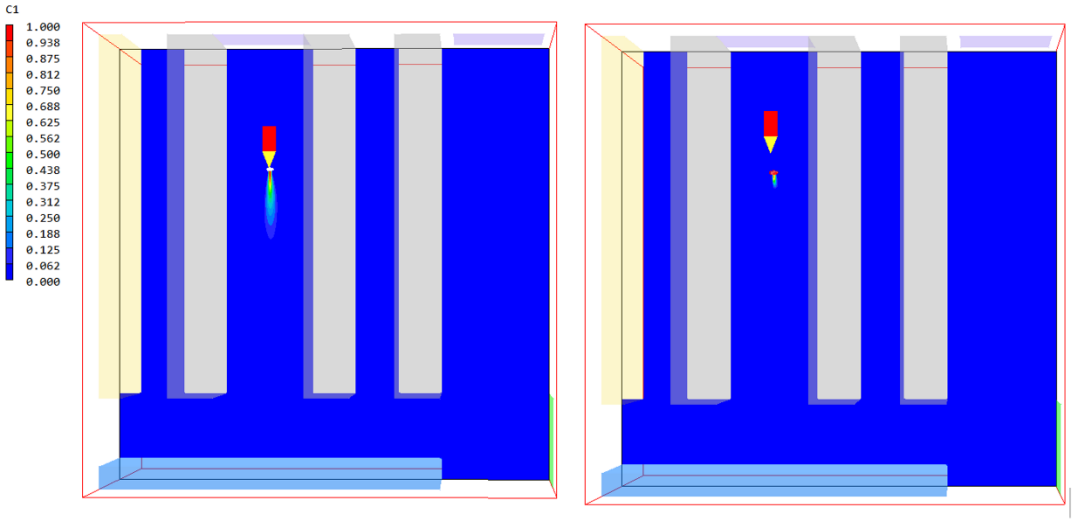

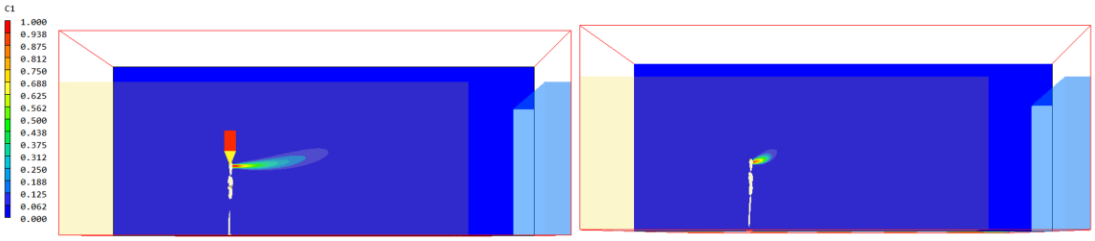


*Figure 30 - Left side: Covid Patient - Right Side: Asymptomatic Covid Patient*

### 4.5.4. Asymptomatic patient study at model 1 – Worst case scenario

Two separate simulation was contacted in the first Design. The reason that the first design was selected was that had a bigger domain. The purpose of this section is to verify the existence of small concentration values, coming from asymptomatic patient breathing, in long distance. In the present section the vectors that are examined are not perpendicular to the ground of the domain, on the contrary they have the direction in which the concentration tends to have large values (worst case).

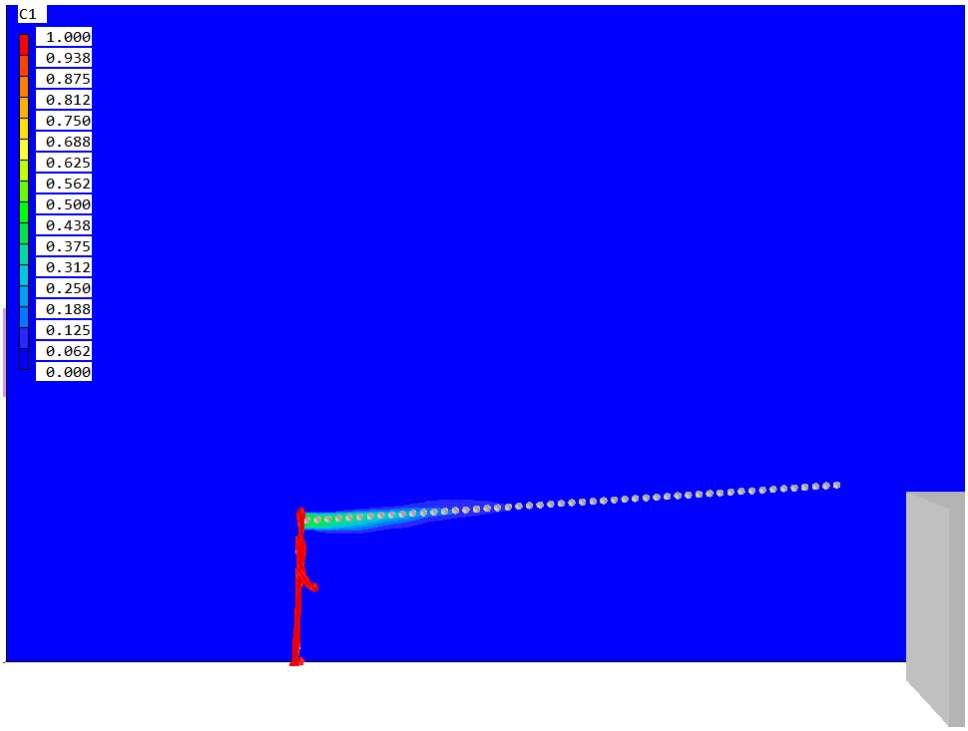


*Figure 31 – Worst case, asymptotic patient study, Vector of concentration that was plotted*

Specifically, the difference of those two simulations is that the one has lower constant value of 40% in the inlet and the second has inlet velocity of 0.4 m/s of the asymptomatic patients face.

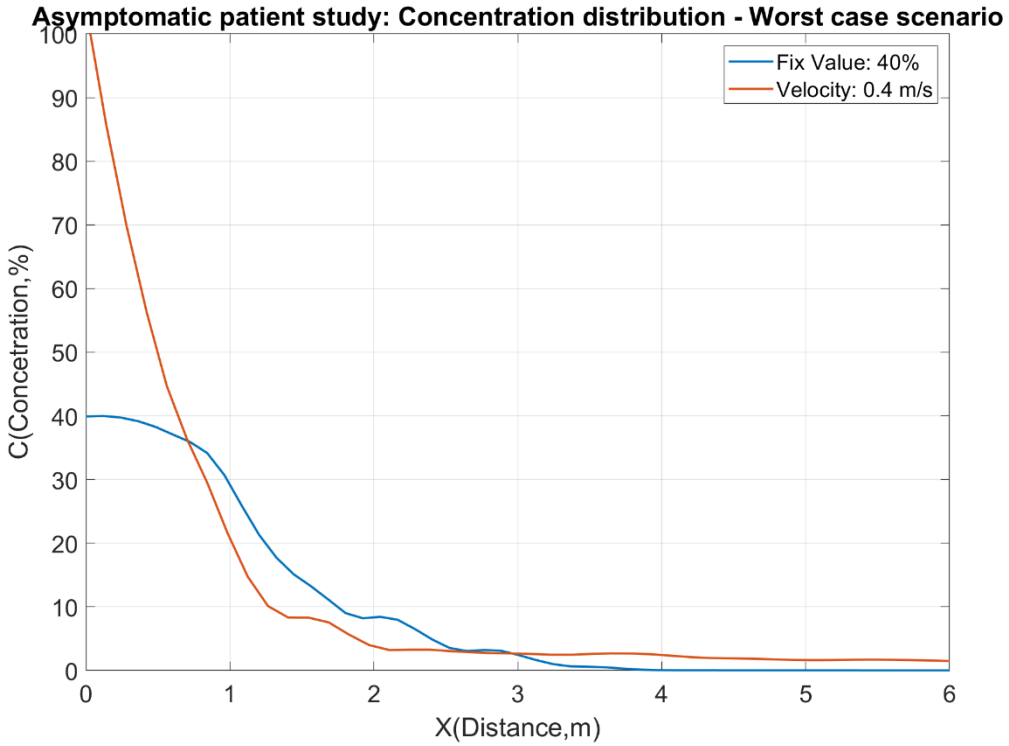


*Figure 32 – Worst case, asymptotic patient study concentration distribution*

The concentration of the first simulation (blue line) at 2.9m is 3.3% while at 5,5m is 0.03%. Furthermore, the concentration of the second simulation (purple line) at 2.9m is 3.1% while at 5,5m is 1.75%

## 5. Limitations

The first limitation is the modeling of the droplets and aerosols. Due to lack of time the droplets and aerosols are simulated as concentration percentage in the air. A more accurate representation would be to simulate the droplets as liquid phase.

## 6. Conclusion

As for today a promising start has being made in the vaccination sector and day by day promising treatments are proposed. Even though the progress in pharmaceutical and vaccination is remarkable given the short time, their effectiveness has yet to be improved. Furthermore, their supply is still limited. Thus, it is still very important to prevent the transmission of the virus as much as

possible. The virus has been proven very contagious and there is strong evidence that it can be transmitted by inhalation of infected saliva in aerosol particles. Creation of those aerosols is due to breathing, talking, laughing, coughing or sneezing.

A big step would be to further reduce the infection due to airborne transmission at the lowest possible level and at the same time make the presence of people in public places as sustainable as can be. This master thesis investigation was conducted to offer understanding of the airflow patterns in public places. The goal has been carried out to investigate the transmittance distance of the airborne infectious particles.

The current social distancing regulation does not take into account possible aerodynamics effects that may cause due to A/C, windows and doors. A ventilated internal space without a mask can be seen as a situation that people should avoid. In those cases, the concentration was bigger than 10 % until 3 m and it seems safer after 6 m. The second design has shown that A/C in its higher operation fan speed enables significantly high concentration values at the distance between 1 and 3 m. Thus, the high fan operation speed cannot be recommended. Mixed are the results that connect the concertation with the temperature of A/C unit, a steady conclusion cannot be made in those cases. Finally, the case does not include A/C units has shown less than 10 % after 1.65m that may justify the current regulation that indicates 1.5 m for safe distance while wearing a mask.

As for the case that involved an asymptotic patient. The small concentration that is present in 5 meters is a proof of the risk of being exposed to Covid-19 indoors can be greater than the 2 m of the Greek and 6 feet (1.82 m) of the American guidelines indicate. This small concentration can be interpreted as small droplets that come from people's warm exhalation and affected by air currents (Air-condition in the present study) can travel throughout the room elevating the risk of airborne transmission. This study does not take masks into consideration. The last case that involved an asymptotic patient made this study more realistic considering that the bigger droplets which are produced by sneezing and coughing are the ones obstructed by masks whilst in the last case the smaller droplets which are produced by breathing are not obstructed by masks.

For the purpose of emphasizing the guidelines that were developed specifically to mitigate the risk of long-range airborne transmission, it must be noted that 6 feet away from another person may not be enough when people are indoors for prolonged periods of time.

Airborne pathogens can be accumulated whilst the asymptomatic patients remain in the same room. Excluding the distance of 1.5 m which was deemed high-risk with higher transmission possibilities compared to the other distances between 6 feet or even 30 feet which similarly have smaller but still existent possibilities of transmission of Covid-19 pathogens. Thus, there is a margin for scientific research of ways where adequate ventilation can contribute to the reduction of the small concentration in internal environment with relatively greater occupancy. Many guidelines are focusing on late night curfew and other strict measures complacent that the 6 feet distance rule will prevent the transmission. At the same time there should be no confusion for the citizens that it is safer to congregate safely within 6 feet distance when in reality there is risk of transmission even in 30 feet distance. In order for public gatherings to be sustainable citizens should meet up in external spaces or in internal spaces where there are air purifiers or air sanitizers.

## 7. Acknowledgement

I wish to express my sincerest gratitude and warm appreciation to the following persons who had contributed much in helping of the final product of the work.

Dr. Nicholas Markatos, for showing great patience with me and teaching me fundamentals of CFD and for the fact that he tirelessly corrected all my drafts and guiding me along the way.

Dr. Maria Founti, for assuming the responsibility of being my thesis advisor and for her support as well.

My classmate and friend Thodore Chrisoloras, in his help at the results analysis chapter.

My parents, my grandma and my fiancée for their support.

# 8. Future Work

The year 2020 has proven to be a very difficult year due to the pandemic impacts on people's health, economies and difficulties in many aspects of everyday life. Further studies can be made to produce an even more realistic representation of the public places' sustainability. As for the example models that would include the addition of masks and face shields. Also, simulation that would treat jet of droplets coming out as separate phase aerosols.

A model that is including A/C units with fins that would guide the air has been created, although due to the lack of time it has not been fully researched.

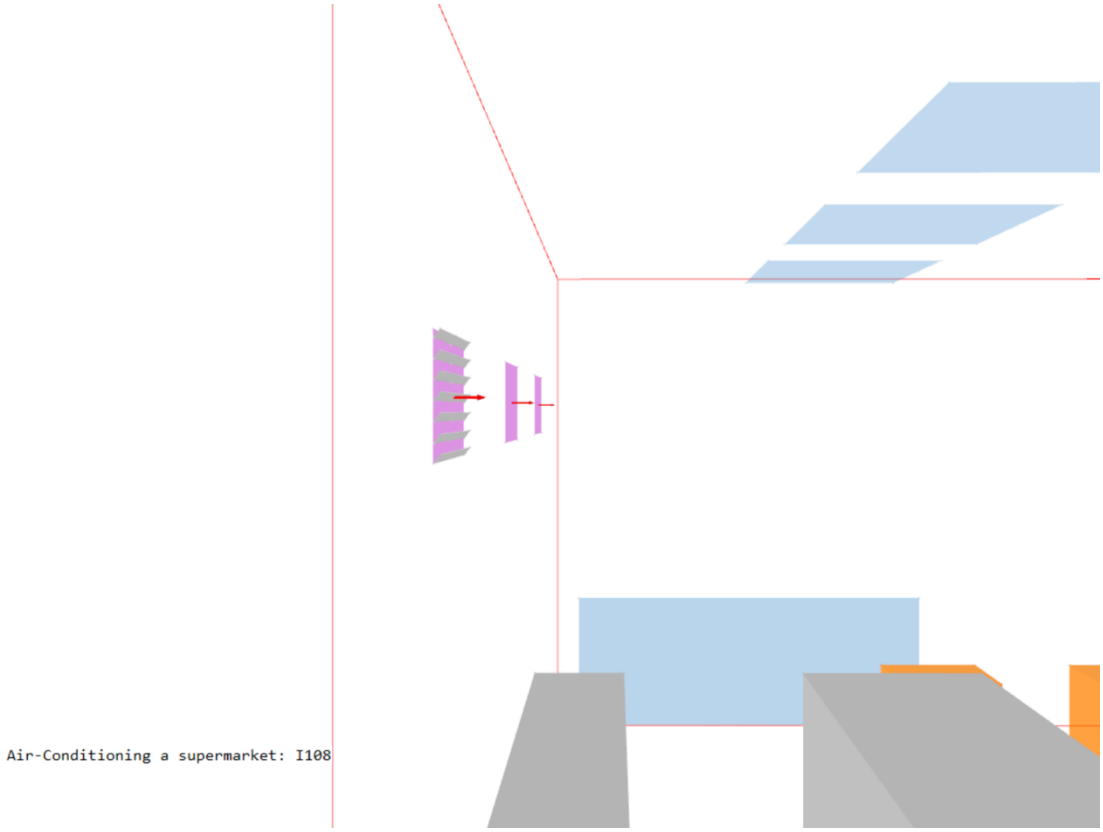


*Figure 33 - Fins in A/C for guided airflow*

# 9. Reference

[1] Xia Yang, Cuiyun Ou, Hongyu Yang, Li Liu, Tie Song, Min Kang, Hualiang Lin, Jian Hang, Transmission of pathogen-laden expiratory droplets in a coach bus, Journal of Hazardous Materials, Volume 397, 2020, 122609, ISSN 0304-3894

[2] Dhand, Rajiv & Li, Jie. (2020). Coughs and Sneezes: Their Role in Transmission of Respiratory Viral Infections, Including SARS-CoV-2. American Journal of Respiratory and Critical Care Medicine. 202. 10.1164/rccm.202004-1263PP.

[3] van Doremalen N., Bushmaker T., Morris D. H., et al. Aerosol and Surface Stability of SARS-CoV-2 as Compared with SARS-CoV-1. *N. Engl. J. Med.* 2020;382:1564–1567. doi: 10.1056/NEJMc2004973.

[4] Reinders Folmer, Christopher & Kuiper, Malouke & Olthuis, Elke & Kooistra, Emmeke & de Bruijn, Anne & Brownlee, Megan & Fine, Adam & Van Rooij, Benjamin. (2020). Compliance in the 1.5 Meter Society: Longitudinal Analysis of Citizens' Adherence to COVID-19 Mitigation Measures in a Representative Sample in the Netherlands in Early April, Early May, and Late May. SSRN Electronic Journal. 10.2139/ssrn.3624959.

[5] Patel, Ashwanee & Dhakar, P.. (2018). CFD Analysis of Air Conditioning in Room Using Ansys Fluent. 10.13140/RG.2.2.13462.50249.

[6] CHAM Ltd, London, UK (2019), PHOENICS (CFD simulation software)

[7] Wilcox, D. C. (1988). Re – assessment of the scale – determining equation for advanced turbulence models. AIAA Journal (Vol. 26, pp. 1299 – 1310). AIAA.

[8] Wilcox, D. C. (2008). Formulation of the k – ω Turbulence Model Revisited. AIAA Journal (Vol. 46, pp. 2823 – 2838). AIAA.

[9] Prandtl, L. (1925). "Z. angew". Math. Mech. 5 (1): 136–139.

[10] Versteeg, H. K., and Malalasekera, W. (2007). An Introduction to Computational Fluid Dynamics: The Finite Volume Method. Pearson Education Limited.

[11] Yakhot, V., Orszag, S.A., Thangam, S., Gatski, T.B. & Speziale, C.G. (1992), "Development of turbulence models for shear flows by a double expansion technique", Physics of Fluids A, Vol. 4, No. 7, pp1510-1520.

[12] Y.S. Chen, S.W. Kim, Computation of turbulent flows using an extended k-e turbulence closure model, NASA CR-179204, 1987.

[13] D. Lee, C.L. Yeh, Computation of reacting flame stabilizer flows using a zonal grid method, Numer. Heat Transfer 24 (1993) 173±285.

[14] Stone, H. L. (1968). "Iterative Solution of Implicit Approximations of Multidimensional Partial Differential Equations". SIAM Journal on Numerical Analysis. 5 (3): 530–538. doi:10.1137/0705044. hdl:10338.dmlcz/104038

[15 J C Ludwig (2020) "PHOENICS – Your Gateway to CFD Success Documentation for PHOENICS |TR 006", CHAM Ref: CHAM/TR006, Software version: PHOENICS 2020v1.0

[16] Saad, Yousef & Yeung, M. & Erhel, Jocelyne. (1998). A deflated version of the Conjugate Gradient Algorithm. SIAM Journal on Scientific Computing. 21.

[17] Tang JW, Nicolle AD, Klettner CA, et al. Airflow dynamics of human jets: sneezing and breathing - potential sources of infectious aerosols. PLoS One. 2013;8(4):e59970. doi:10.1371/journal.pone.0059970